Spectrochimica Acta Part A: Molecular and Biomolecular Spectroscopy 363 (2026) 128311

Contents lists available at ScienceDirect

Spectrochimica Acta Part A:
Molecular and Biomolecular Spectroscopy

journal homepage: www.journals.elsevier.com/spectrochimica-acta-part-a-molecular-and-biomolecular-spectroscopy

DFT insights into dopamine adsorption on pristine and Ag-doped carbon nanotubes: implications for SERS sensing applications

Jamelah S. Al-Otaibi [a,*], Y. Sheena Mary [b], Y. Bhargav Kumar [c], Kaippallil S. Resmi [d], Gaurav Jhaa [e], Maria Cristina Gamberini [f]

[a] Department of Chemistry, College of Science, Princess Nourah Bint Abdulrahman University, P.O. Box 84428, Riyadh 11671, Saudi Arabia
[b] Department of Physics, FMN College (Autonomous), Kollam, Kerala, University of Kerala, India
[c] Department of Polymers and Functional Materials, CSIR-Indian Institute of Chemical Technology, Hyderabad, India
[d] Department of Physics, KCG College of Technology, Karapakkam, Chennai, Tamil Nadu, India
[e] Department of Chemical Sciences, Indian Institute of Science Education and Research (IISER) Mohali, Punjab, India
[f] Department of Life Sciences, University of Modena and Reggio Emilia, via G. Campi 103, 41125 Modena, Italy

HIGHLIGHTS

- Ag doping greatly enhances dopamine adsorption on CNTs through stronger charge transfer and orbital coupling.
- CNTAgNH2 shows the strongest adsorption and highest thermodynamic stability.
- DOS, FMO, NCI, and RDG analyses confirm improved electronic interaction after Ag doping.
- Raman and IR shifts indicate strong coupling and SERS potential for dopamine sensing.

GRAPHICAL ABSTRACT

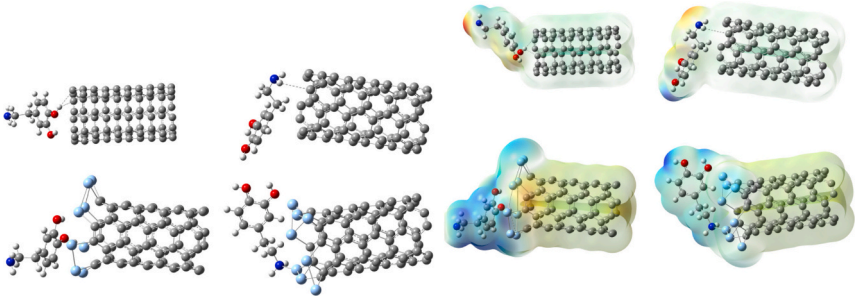

ARTICLE INFO

Keywords:
DFT
Dopamine
Carbon nanotubes
Adsorption
SERS

ABSTRACT

In this work, DFT was used to investigate the adsorption behaviour of dopamine on pristine and Ag-doped carbon nanotubes. Two adsorption orientations, involving hydroxyl and amine groups of dopamine, were examined to clarify role of functional-group direction in molecule-surface interactions. The results show that Ag doping strongly enhances dopamine adsorption by increasing charge transfer, surface polarization, and orbital coupling. Among the studied systems, $CNTAgNH_2$ exhibited strongest adsorption energy, highest dipole moment, and most favourable thermodynamic stability, indicating strong Ag-mediated interaction through amine group. FMOs, MEP, DOS, NCI, and RDG analyses further confirmed that Ag incorporation narrows the electronic gap and introduces active interaction sites. Vibrational analysis revealed significant shifts in OH, NH_2, phenyl, and CH_2 modes after adsorption, supporting enhanced chemical interaction and possible SERS signal amplification. Overall, Ag-doped CNTs, particularly the $CNTAgNH_2$ configuration, appear to be promising nanosubstrates for dopamine detection, although very strong adsorption may reduce sensor recyclability.

* Corresponding author.
E-mail addresses: jamelahsalotaibi@gmail.com (J.S. Al-Otaibi), bhargavkumar1804@gmail.com (Y.B. Kumar).

https://doi.org/10.1016/j.saa.2026.128311
Received 19 May 2026; Received in revised form 12 June 2026; Accepted 22 June 2026
Available online 23 June 2026

1. Introduction

Because of their remarkable mechanical strength, high electrical and thermal conductivity, and large specific surface area, carbon nanotubes (CNTs), one-dimensional nanostructures made of rolled graphene sheets, are useful materials for electronics, energy storage, sensors, and catalytic applications. Their sp^2-bonded carbon network and adjustable electronic properties (such as metallic versus semiconducting behaviour) based on tube diameter and chirality give them their special qualities. The vast technical value of CNTs is highlighted by recent reviews that continue to emphasize continuous advancements in CNT synthesis, purification, functionalization, and integration into diverse systems ranging from batteries to nanoscale electronics [1].

Coinage metals (Cu, Ag, and Au) and related hetero atoms can be doped into carbon nanotubes to modify their electrical, catalytic, and adsorption characteristics. It has been demonstrated that adding Cu and N into CNTs greatly changes the electronic density of states and improves electrical conductivity, especially in semiconducting CNTs with nitrogen functional groups [2]. Cu-doped CNTs can enhance interactions with adsorbates like hydrogen, according to first-principles and DFT research, indicating promise for hydrogen storage materials [3]. Coinage metal doping can open up new possibilities for energy storage applications, as Au-doped CNTs have been anticipated to boost hydrogen uptake capacities at elevated temperatures [4]. Beyond energy, co-doping single-walled CNTs with Au, Ag, or Cu in addition to hetero-atoms (such B or N) can alter adsorption energies and selectivity, which is important for sensing and separation technologies [5]. When taken as a whole, our investigation suggest that coinage metal-doped carbon nanotubes represent a viable class of tailored nanomaterials with customizable functional capabilities driven by regulated dopant incorporation and electronic structure alteration.

DFT, which offers atomistic insight into binding energetic, electronic structure modulation, and adsorption mechanisms crucial for creating efficient nanotube-based drug delivery systems, has emerged as a potential computational tool for clarifying the basic interactions between CNTs and drug molecules. As demonstrated by anticancer medications like Gemcitabine on Pd-doped single-walled CNTs and droxidopa on COOH-functionalized CNTs, where negative binding energies confirm favourable drug-nanotube complexation, recent DFT studies show that drug adsorption on pristine or functionalized CNTs is usually exothermic with appreciable binding energies, indicating strong physisorption driven by π-π stacking, hydrogen bonding, and van der Waals forces [6,7]. Additionally, research shows that functionalization techniques, like carboxylation or bio-conjugation with targeting ligands like folic acid or hyaluronic acid, can dramatically change HOMO–LUMO gaps and molecular electrostatic potentials, which support better electronic interactions with therapeutic agents such as platinum-based chemotherapeutics, in addition to improving drug affinity and specificity [8,9]. When taken as a whole, these DFT investigations offer comprehensive quantum-level characteristics (such as binding energy, charge transfer, frontier orbital analysis) that are crucial for anticipating and refining CNT–drug interactions for focused and effective drug delivery applications [10].

A thorough atomistic knowledge of dopamine interactions with Ag-doped carbon nanotubes is still lacking, despite the fact that dopamine adsorption on carbon nanomaterials and the SERS activity of silver-based nanostructures have been studied independently. While computational SERS research have mostly looked at dopamine interacting with isolated Ag clusters rather than metal-doped substrates, previous DFT studies primarily concentrated on dopamine adsorption on pristine CNTs, where mild physisorption was found to predominate. Further experimental research shows that adding metallic nanostructures can greatly enhance dopamine sensing performance; however, it has not been thoroughly investigated how Ag dopants affect dopamine's adsorption orientation, charge transfer, electronic structure, and vibrational responses on CNTs. To determine the connection between Ag doping, the adsorption mechanism, and SERS-relevant electrical and vibrational properties, a thorough first-principles study is therefore required [11–14].

Strong hydrogen bonding, π-π stacking, metal coordination, and electrostatic interactions are made possible by dopamine (3,4-dihydroxyphenethylamine), a redox-active catecholamine neurotransmitter with two contiguous hydroxyl groups on a benzene ring and a main amine side chain [15]. It is extremely relevant for surface chemistry and bio-sensing applications due to its oxidation to dopamine-quinone under physiological or electrochemical circumstances. Through π-π interactions between the aromatic catechol ring and sp^2-hybridized carbon surfaces, dopamine shows a strong affinity for carbon-based nanostructures like graphene or carbon nanotubes at the nanoscale [16]. These interactions are frequently accompanied by charge transfer, which alters the electronic properties of the nanomaterial. Additionally, dopamine can also self-polymerize to create polydopamine coatings that stick firmly to oxides, metals and polymeric nanoparticles, offering a flexible platform for drug loading and surface functionalization [17]. Furthermore, its catechol moiety enhances catalytic activity or sensing performance by forming coordination complexes with metal and metal-oxide nanostructures (such as Au, Fe_3O_4, TiO_2). Dopamine is a crucial chemical in brain interfaces, targeted drug delivery systems, nanobiosensors, and bio-inspired surface engineering because of these interaction processes [18,19].

2. Methods

Vibrational frequency calculations were carried out using Gaussian 16 to confirm the nature of stationary points, and NCI analysis based on the RDG was subsequently performed using Multiwfn [20–23]. Using the range-separated hybrid functional wB97XD in conjunction with a mixed basis set scheme def2-TZVP for carbon atoms and an effective core potential (ECP) basis such as def2-ECP for the Ag dopant – is an appropriate theoretical level for studying Ag-doped carbon nanotubes. When used with wB97XD, the def2-TZVP basis, which is a member of Ahlrichs family, offers triple-ζ quality with polarization functions and has been widely suggested for accurately modelling dispersion-dominated systems and non-covalent interactions [24]. The ωB97X-D functional was chosen because it accurately treats both charge-transfer and dispersion interactions, which are crucial in molecule-CNT adsorption processes, by combining long-range-corrected exchange with an empirical dispersion correction. The ωB97X-D offers accurate interaction energies for noncovalent and dispersion-dominated systems, according to earlier benchmark investigations. Furthermore, ωB97X-D has been effectively used in a number of adsorption investigations utilizing pristine and metal-doped carbon nanotubes, precisely describing sensing features, electronic-structure alterations, and adsorption energies. For the current CNT adsorption systems, the ωB97X-D/def2-TZVP framework was thought to provide a suitable balance between computational cost and accuracy [25–28].

ECP-based basis sets are especially useful for large nano-structured systems like doped CNTs since they are crucial for including scalar relativistic effects for heavy transition metals like Ag while drastically lowering computing costs [24]. Because of its effectiveness and proven performance in transition-metal DFT calculations, where it replaces core electrons with an effective potential and permits tractable treatment of massive systems, def2-ECP is still a frequently used option in this context [29]. Double-ζ ECP basis sets are frequently employed in conjunction with triple-ζ basis sets on the lighter atoms to reach a balanced accuracy-cost ratio, despite the fact that they may be less accurate than higher-ζ alternatives. However, their performance can be enhanced by polarization and diffuse functions [30]. For modelling the structural, electronic, and adsorption characteristics of Ag-doped carbon nanotube systems, the wB97XD/def2-TZVP (C) with def2-ECP or LANL2DZ (Ag) level of theory provides a dependable computationally effective framework. It should be mentioned that neither supercell nor periodic

boundary conditions were implemented because the present study employed a finite carbon nanotube cluster model within the Gaussian framework. An isolated zigzag (8,0) carbon nanotube consisting of 80 carbon atoms, with optimized dimensions of 5.47 Å in diameter and 11.90 Å in length, was adopted for all calculations. Finite CNT models are widely used in Gaussian-based adsorption and sensing studies because they provide a computationally efficient representation of localized adsorbate–nanotube interactions while accurately capturing the essential electronic characteristics of the nanotube. Furthermore, nanotube chirality, diameter, and size are known to strongly influence adsorption behaviour and electronic properties; therefore, these structural parameters were carefully selected and explicitly considered to ensure the reliability and reproducibility of the adsorption and electronic-structure analyses [31–33]. Since the singlet ground state (multiplicity = 1) was used for all calculations, a restricted Kohn–Sham DFT formalism was used. The ωB97X-D functional was chosen because it accurately describes long-range charge-transfer and van der Waals interactions, which are crucial for simulating adsorption processes on doped carbon nanostructures, when combined with empirical dispersion corrections [25]. Because of its triple-ζ quality and demonstrated dependability for electronic-structure calculations, the def2-TZVP basis set was used for light atoms, whereas the matching def2 effective core potential was used to represent Ag in order to effectively account for scalar relativistic effects [34,35]. This combination offers a useful trade-off between computational precision and cost, and it has been extensively employed in research on transition-metal-containing nanomaterials and adsorption systems [36]. The intrinsic interactions between dopamine and the Ag-doped CNT in the absence of solvent effects are described by the current computations, which were carried out in the gas phase. The current method offers a basic understanding of the adsorption mechanism at the molecular level, even though aqueous conditions may affect adsorption behaviour through solvation and hydrogen-bonding interactions. Furthermore, although BSSE adjustments were not specifically assessed, it is anticipated that using the triple-ζ def2-TZVP basis set will reduce BSSE in comparison to smaller basis sets. Dynamic and anharmonic temperature effects were not taken into account because thermodynamic parameters were determined inside the harmonic oscillator approximation at 298.15 K [34].

Two adsorption configurations were explored in this study, where the hydroxyl groups and the NH_2 group of dopamine were positioned close to the termini of pristine and Ag-doped carbon nanotubes, denoted as CNTAgOH and $CNTAgNH_2$, respectively, to evaluate their adsorption behaviour. Fig. 1 gives the structure, FMOs and MEP of dopamine. The optimized geometries of CNT & Ag doped CNT, $CNTOH/NH_2$ & $CNTAgOH/NH_2$ are shown in Fig. S1 and Fig. 2. The recovery time (τ) of the adsorbed drug molecule was calculated using transition-state theory in order to assess the regeneration capability of the suggested CNT-based sensing platform. The formula is $\tau = \upsilon^{-1}$ exp. (−Eads/kT), where τ is the recovery time (s), υ is the attempt frequency of the desorption process, Eads is the adsorption energy, k is the Boltzmann constant, and T is the absolute temperature. Desorption barrier was determined by the absolute value of Eads because it is negative for spontaneous adsorption. Recovery time is a crucial metric for evaluating sensor reusability since it given an approximation of the analyte's residence period on the nanotube surface. Strong enough adsorption to allow detection while allowing desorption and regeneration of the sensor substrate is indicated by moderate recovery times. The adsorption energies derived from DFT calculations were used in this investigation to compute recovery durations at 400 K [37].

3. Results and discussion

3.1. Adsorption properties

The computed electronic characteristics shown in Table 1 shed light on the systems under study's stability, charge distribution, and interaction strength. The virgin drug molecule (0516.49 Hartree) is substantially less stable than the nanotube-based systems, according to the total electronic energies, although functionalization and metal decorating show gradual stability. The Ag-decorated complexes, in particular, show the highest negative energies; the most stable configuration is $CNTAgNH_2$ (−4434.50 Hartree), indicating a significant interaction between the drug and the modified nanotube surface. This behaviour is in line with density functional theory (DFT) research that demonstrates how metal ornamentation increases adsorption via orbital hybridization and charge transfer mechanisms [38,39]. Significant charge redistribution during adsorption is also supported by the dipole moment values. Ag ornamentation significantly raises the dipole moment (18.43 Debye), which increases further following drug adsorption to reach 29.61 Debye for $CNTAgNH_2$. In contrast, the virgin nanotube is almost nonpolar (0.01 Debye). This rise suggests stronger intermolecular contacts and increased polarity, especially for the amine-functionalized system, which is known to operate as an electron-donating group that facilitates charge transfer [40]. Additionally, polarizability rises significantly from 93.51 a.u. for the isolated drug to 774.63 a.u. for the nanotube and achieves a maximum of 1446.75 a.u. for CNTAgOH. Increased electronic cloud distortion in bigger π-conjugated systems and metal-modified nanostructures is seen in this trend. According to earlier studies on functionalized carbon nanomaterials, the OH-functionalized complex's marginally higher polarizability indicates improved electron delocalization in comparison to the NH_2 counterpart [41]. The hyperpolarizability values show a significant improvement, rising from 11.81 a.u. for the pristine nanotube to 39,567.77 a.u. for the Ag-decorated system. The Ag-containing complexes, especially $CNTAgNH_2$ (31,467.43 a.u.), maintain very high hyperpolarizability despite drug adsorption lowering this value, indicating a significant nonlinear optical (NLO) response. Such phenomenon has been extensively documented in recent NLO research and results from effective charge transfer and donor–acceptor interactions in metal–nanotube hybrids [42].

Positive interactions between the drug and nanotube systems are

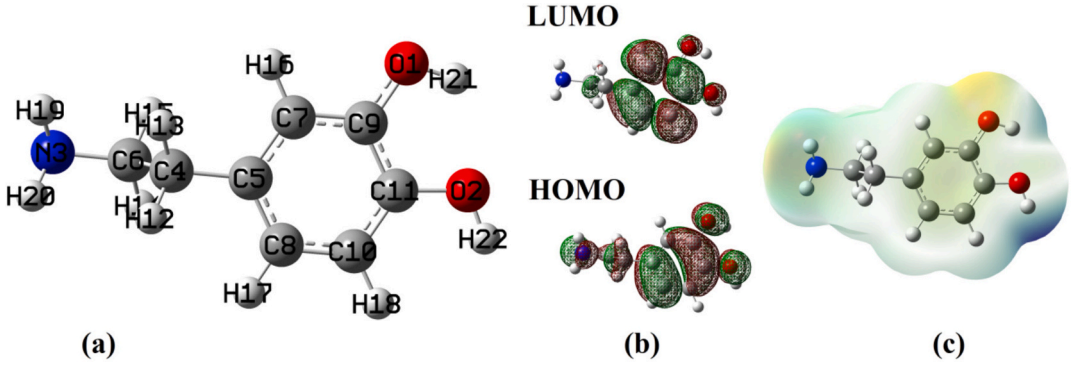

Fig. 1. Dopamine's (a) optimized structure (b) FMOs (c) MEP plots.

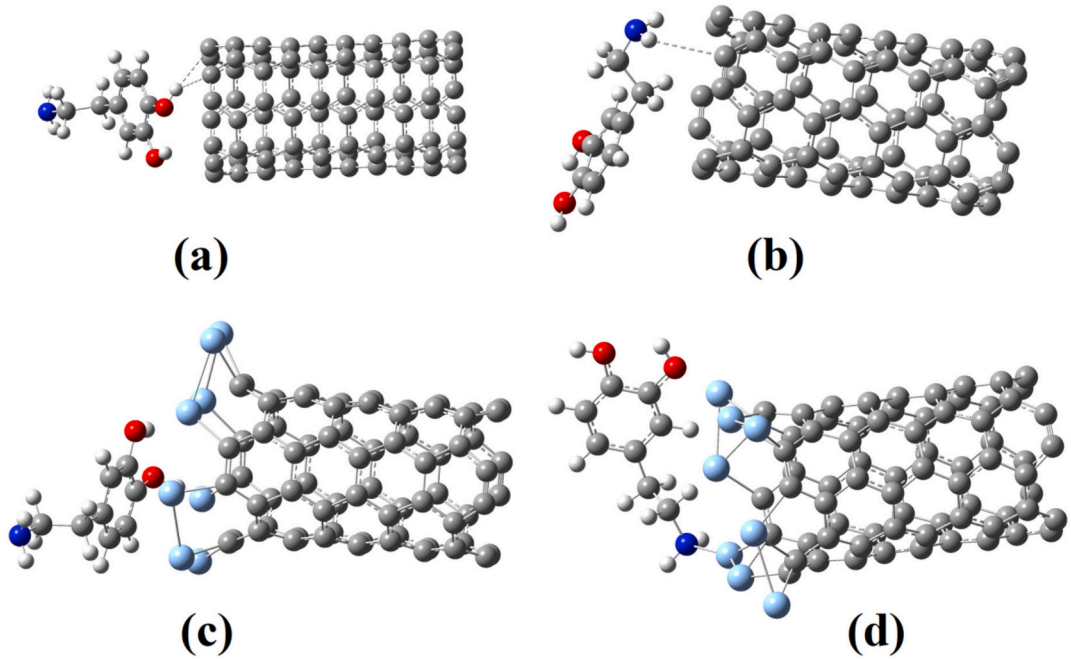

Fig. 2. Optimized structures of (a) CNTOH (b) $CNTNH_2$ (c) CNTAgOH (d) $CNTAgNH_2$.

Table 1
Energies, dipole moment, polarizability, hyperpolarizability and adsorption energies.

Systems	Energy (Hartree)	Dipole moment (Debye)	Polarizability (a.u.)	Hyper polarizability (a.u.)	Adsorption energy (kcal mol^{-1})
Dopamine	−516.492802	2.98	93.51	210.72	–
CNT	−3046.369781	0.01	774.63	11.81	–
CNTAg	−3917.933362	18.43	1145.74	39,567.77	–
CNTOH	−3562.883385	3.37	902.48	5867.97	−13.05
$CNTNH_2$	−3562.880551	3.60	892.27	3548.65	−11.28
CNTAgOH	−4434.469238	17.91	1446.75	11,815.74	−27.03
$CNTAgNH_2$	−4434.498280	29.61	1228.32	31,467.43	−45.25

confirmed by the adsorption energies. Ag-decorated systems exhibit much stronger adsorption (−27.03 and −45.25 kcal mol^{-1}), while the virgin nanotube displays modest adsorption energies (−13.05 and −11.28 kcal mol^{-1}), which are indicative of physisorption. $CNTAgNH_2$'s extremely low value indicates that partial chemisorption, most likely as a result of coordination between the amine group and Ag atoms. This increased binding strength is in line with computer research showing that metal doping dramatically raises interaction stability and adsorption energies [43]. While functional groups further influence the interaction, Ag ornamentation generally plays a major role in improving stability, adsorption strength, and electronic characteristics. Because of its strong binding, high dipole moment, and remarkable NLO features, the $CNTAgNH_2$ system stands out as the most promising option; however, overly strong adsorption may impact drug release behaviour.

In addition to the complexes' thermodynamic stability, the adsorption process significantly alters the nanotube surface's electrical structure. Orbital hybridization between the Ag 4d states, the CNT's π-electron network, and dopamine's frontier orbitals is responsible for the increased adsorption seen in the Ag-decorated systems. The significant rise in dipole moment and polarizability after adsorption indicates that such hybridization promotes interfacial charge transfer. Specifically, the $CNTAgNH_2$ complex demonstrates effective electronic communication between the adsorbate and substrate by combining high adsorption (−45.25 kcal mol^{-1}) with considerable electronic polarization. It is anticipated that these adsorption-induced electronic perturbations will change the nanotube's charge-carrier density and conductivity, producing a detectable sensing signal. Therefore, among the systems under investigation, $CNTAgNH_2$ is the most promising option for dopamine sensing due to its high polarization response, improved charge redistribution, and superior adsorption strength.

3.2. Chemical descriptors

Dopamine's HOMO-LUMO analysis shows a comparatively large energy gap of 5.43 eV, indicating low inherent chemical reactivity and excellent kinetic stability in its isolated form (Table S1). Significant π-electron delocalization across the phenyl framework is reflected in the highest occupied molecular orbital (HOMO), which is mostly located over the aromatic ring and partially extends toward the hydroxyl substituents (Fig. 1b). The LUMO, on the other hand, is primarily dispersed throughout the aromatic ring with a discernible expansion toward the amine (NH_2) group, indicating that electron acceptance is preferred in these areas. A possible charge-transfer pathway from the electron-rich phenyl moiety to the electron-deficient areas involving the amine group is highlighted by the spatial difference between HOMO and LUMO densities. Dopamine acts as a moderately stable molecule with little reactivity unless disturbed by external interactions like adsorption or coordination with metal sites, as seen by the huge HOMO–LUMO gap (5.43 eV), which equates to low polarizability and decreased electrical conductivity [44].

Dopamine's molecular electrostatic potential (MEP) surface sheds light on the molecule's reactive sites and charge distribution (Fig. 1c) [45]. Strong electron-rich centers that are advantageous for electrophilic attack and hydrogen bonding interactions are found mostly

around the oxygen atoms of the hydroxyl groups, which are the regions with the largest negative electrostatic potential (usually shown by red to orange tints). Due to π-electron delocalization, a moderate negative potential is also seen across some of the aromatic ring. On the other hand, the hydrogen atoms of the amine (NH_2) group, to a lesser extent, the hydrogen atoms of the hydroxyl groups are primarily surrounded by regions of positive electrostatic potential (blue shades) indicating their potential importance as sites for nucleophilic interactions. A balanced charge distribution is reflected in the central carbon framework's comparatively neutral potential (green to light yellow areas). Dopamine's overall MEP profile reveals a clear polarity, with electron density concentrated at the hydroxyl functionalities and electron-deficient areas surrounding the amine hydrogens, which together control its reactivity and intermolecular behaviour in complex environments [46].

3.2.1. CNT and CNT-Ag's FMOs

Significant changes in the electrical structure upon metal inclusion are revealed by the HOMO–LUMO analysis of the virgin carbon nanotube (left panel) and Ag-doped carbon nanotube (right panel) (Fig. S2). With an energy gap of 4.48 eV that reflects its semiconducting nature and moderate chemical durability, the virigin nanotube's the HOMO and LUMO are largely delocalized over the π-conjugated carbon framework, showing uniform electron dispersion over the tube surface. The Ag-doped nanotube, on the other hand, shows a similar energy gap of 3.87 eV, indicating improved reactivity and electrical conductivity. Strong orbital hybridization and charge redistribution brought on by the dopant are seen in the border molecular orbitals in the doped system, which clearly localize around the Ag atoms and nearby carbon sites. The LUMO covers both the metal and the nanotube surface, allowing for potential charge transfer interactions, whereas the HOMO density is partially localized close to the Ag centers. Ag doping dramatically changes the electronic characteristics of the nanotube, making it more advantageous for adsorption and sensing applications, as confirmed by the localized electrical features and the band gap reduction (by about 0.61 eV) [47].

3.2.2. CNT and CNT-Ag's MEP

The pristine carbon nanotube and the Ag-doped nanotube's molecular electrostatic potential (MEP) maps clearly demonstrate how doping affects charge distribution (Fig. S3). The electrostatic potential in the pristine nanotube is smoothly spread over the whole π-conjugated carbon structure, suggesting low polarization and delocalized electron density. Its' chemically robust and less reactive nature is reflected in the very minor alterations seen, with faint positive regions close to the outer hydrogen atoms and weakly negative regions dispersed throughout the carbon network. The Ag-doped nanotube, on the other hand, displays a clearly non-uniform potential distribution, with a strong localization of negative potential around the Ag atom and its nearby carbon atoms, while surrounding areas exhibit enhanced positive character. Strong polarization brought on by the metal dopant is indicated by this charge redistribution, which results in the creation of active sites on the surface of the nanotube. When compared to the pristine nanotube, these localized electrostatic characteristics improve the doped system's capacity to interact, making it more advantageous for adsorption and surface reactivity [48].

3.2.3. CNTOH/NH_2 FMOs & MEP

Depending on the direction of the functional group, the HOMO–LUMO distributions of the carbon nanotube–dopamine complexes show different interaction properties (Fig. 3). Both the HOMO and LUMO densities are mostly delocalized over the carbon nanotube's π-framework in the configuration where the dopamine OH group is close to the nanotube, with the dopamine moiety contributing very little. This shows poor electronic coupling and implies that van der Waals and non-covalent π-π interactions dominate the interaction. On the other hand, a discernible extension of the frontier molecular orbitals toward the dopamine fragment is seen when the NH_2 group of dopamine is directed toward the nanotube, especially in the HOMO. Stronger electronic contact between the nanotube and the amine group is implied by this partial orbital overlap, which promotes charge transfer interactions. In this form, the LUMO exhibits a small disturbance close to the contact

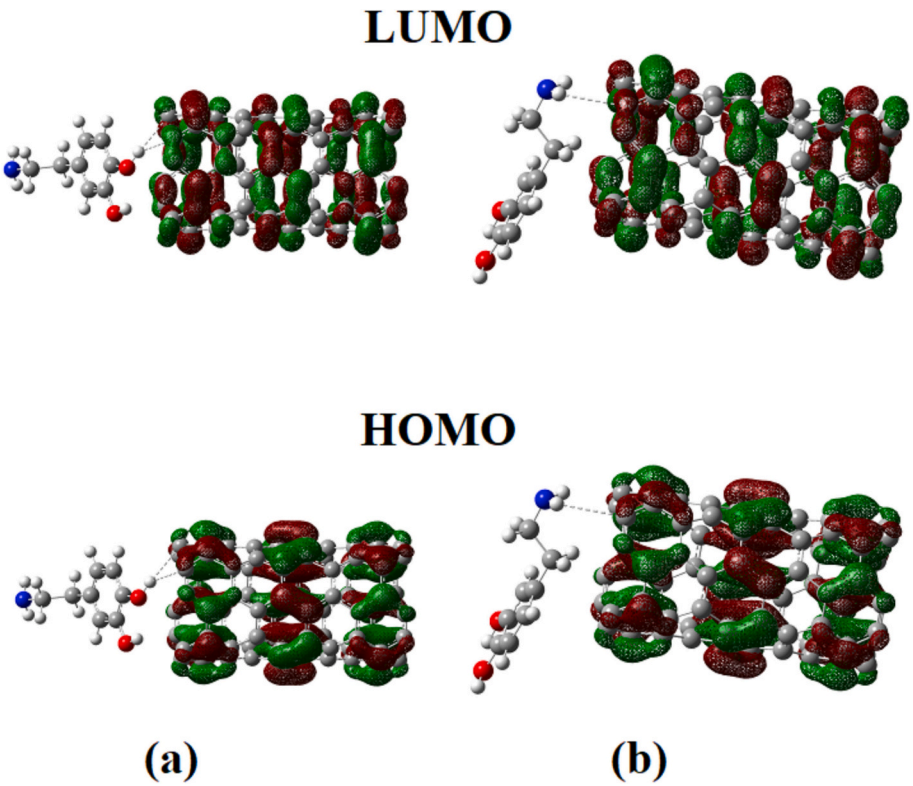

Fig. 3. FMOs of (a) CNTOH (b) $CNTNH_2$.

group, although it is still primarily concentrated on the nanotube. Overall, the findings show that the NH_2 group encourages higher electrical contact than the OH group, which could affect the nanotube system's sensing behaviour and adsorption strength [49].

The charge distribution and preferred interaction sites for various functional group orientations are revealed by the molecular electrostatic potential (MEP) maps of the carbon nanotube–dopamine complexes (Fig. 4). When dopamine's OH group is placed close to the nanotube, the hydrogen atom has a comparatively positive potential (blue/green region), while the oxygen atom has a strong negative potential (red region). The carbon nanotube's surface stays mostly neutral (green), demonstrating weak polarization and implying that the non-covalent forces like dispersion interactions and hydrogen bonding dominate the interaction. On the other hand, a more noticeable charge separation is seen when the NH_2 group is oriented toward the nanotube, with the hydrogen atoms displaying positive potential and the nitrogen area displaying comparatively negative potential. When compared to the OH arrangement, this causes the next nanotube surface to become somewhat more polarized. Stronger electrostatic contact and potential charge transfer between dopamine and the nanotube are indicated by the wider spread of electrostatic potential in this instance. In general, the MEP analysis indicates that the NH_2 group interacts with the nanotube surface more strongly than the OH group, which is consistent with improved adsorption properties [50].

3.2.4. *CNTAgOH/NH_2 FMOs & MEP*

The frontier molecular orbital distributions shed light on how the dopamine adsorption arrangement affects the Ag-doped carbon nanotube's electrical structure (Fig. 5). With just small contributions from the dopamine moiety, the HOMO is mostly delocalized across the nanotube framework for the OH-oriented configuration, suggesting poor electronic coupling via the hydroxyl group. On the other hand, the LUMO exhibits partial localization close to the adsorption site and the Ag dopant indicating that this contact facilitates charge transfer following excitation. A more noticeable interaction is seen when dopamine is oriented via the NH_2 group: both HOMO and LUMO densities show enhanced overlap between the molecule and the nanotube surface, especially near the Ag atom. Stronger electronic coupling and a more effective charge transfer channel are implied by this increased orbital mixing. Overall, compared to the OH configuration, the NH_2 arrangement seems to encourage more electrical contact with the Ag-doped nanotube, which could have significant effects on charge transport behaviour and sensing performance [37].

The impact of dopamine adsorption on the Ag-doped carbon nanotube is further explained by the molecular electrostatic potential (MEP) surfaces (Fig. 6). With discrete areas of negative potential focused around the oxygen atom and mild polarization close to the Ag dopant, charge dispersion in the OH-oriented structure is comparatively moderate. This implies that dopamine's interaction with the nanotube surface is weaker and that charge redistribution is restricted. The NH_2-oriented form, on the other hand, shows a more noticeable variation in electrostatic potential, with stronger negative areas surrounding the nitrogen atom and increased polarization throughout the nanotube. Increased charge transfer and higher intermolecular interaction mediated by the amine group are shown by the wider and more intense potential gradients. These findings support the frontier orbital analysis and demonstrate the NH2 group promotes more efficient electronic coupling with the Ag-doped nanotube, potentially improving its sensitivity and reactivity in adsorption-based applications.

Based on frontier molecular orbital (FMO) theory, Table S1's chemical reactivity descriptors offer additional information about the pledge systems' stability and electrical behaviour. The drug molecule has the biggest energy gap (Eg = 5.43 eV), indicating strong kinetic stability and low chemical reactivity according to the HOMO (EH) and LUMO (EL) energies. The virgin nanotube, on the other hand, has a smaller band gap (4.48 eV), which further narrows upon Ag decorating (3.87 eV), indicating increased electronic conductivity and reactivity. DFT investigation have frequently documented this decrease in band gap upon metal integration, where metal atoms introduce new electronic states close to the Fermi level, aiding charge transfer processes [51,52].

The global hardness (η), which drops from 2.72 eV for the drug to 1.94 eV for CNTAg, shows a similar pattern, suggesting that metal ornamentation softens the system and increases its chemical reactivity. When compared to the NH_2-functionalized counterpart (1.89 eV), CNTOH shows the lowest hardness (1.61 eV) among the complexes, indicating better reactivity. In line with earlier research on functionalized nanomaterials, decreased hardness is associated with increased polarizability and a greater propensity to engage in charge transfer interactions, according to the principles of conceptual DFT [53,54].

These findings are further corroborated by the chemical potential (μ) values. $CNTNH_2$ displays the least negative value (−2.98 eV), suggesting greater electron-donating ability due to the amine group, while the drug molecule displays the largest negative value (−4.81 eV), indicating significant electron-withdrawing character. Significantly, greater negative potentials (∼ −4.4 eV) are shown by Ag-decorated adsorption systems (CNTAgOH and $CNTAgNH_2$), indicating improved stability and stronger binding interactions. This result is consistent with recent discoveries that metal-doped nanostructures have enhanced adsorption strength and electron-accepting capacity [55].

Further information about the systems' ability to receive electrons is provided by the electrophilicity index (ω). While CNTAg displays a lower value (2.86 eV) showing decreased electrophilic character upon metal ornamentation alone, the pristine drug and nanotube show similar electrophilicity (∼4.2 eV). Nevertheless, the electrophilicity rises once more after drug adsorption, especially for CNTAgH (4.34 eV) and $CNTAgNH_2$ (4.26 eV), indicating that these complexes are potent electrophiles that can stabilize extra electron density. According to recent computational simulations of adsorption mechanisms, this

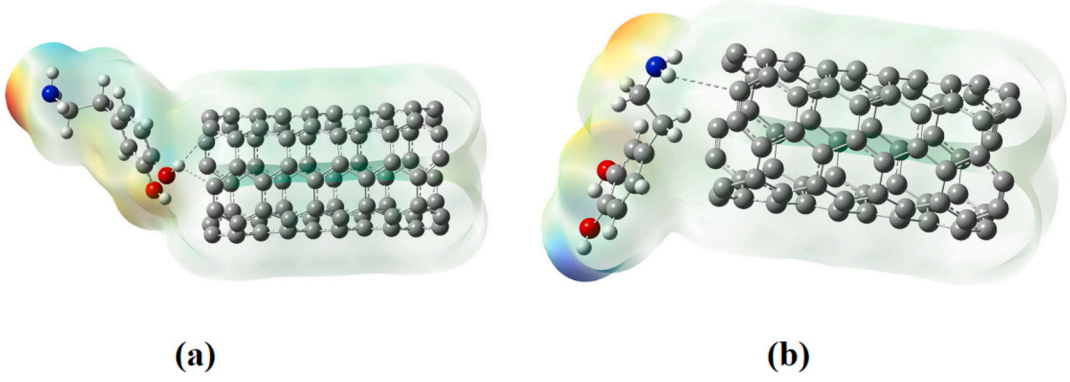

Fig. 4. MEP plots of (a) CNTOH (b) $CNTNH_2$.

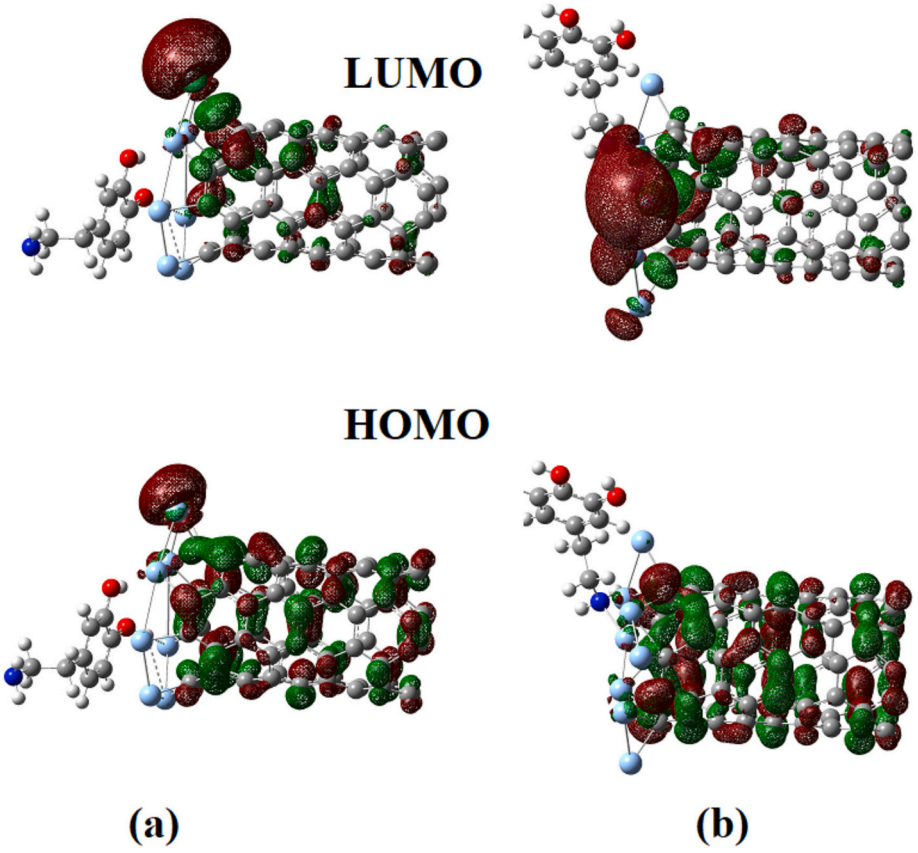

Fig. 5. FMOs of (a) CNTAgOH (b) $CNTAgNH_2$.

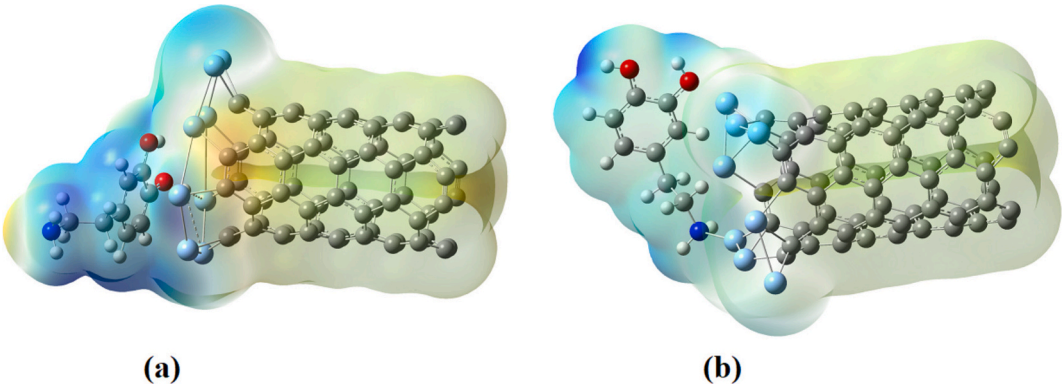

Fig. 6. MEP plots of (a) CNTAgOH (b) $CNTAgNH_2$.

augmentation is compatible with donor-acceptor interactions between the drug molecule and Ag-decorated nanotube [56].

The decrease in the energy gap after Ag decorating is especially important from a sensing standpoint since it indicates more electronic conductivity and a higher vulnerability of the nanotube to outside disturbances. Preferential adsorption centers that can be effectively interact with dopamine through charge-transfer mechanisms are created by the localization of frontier molecular orbitals around the Ag active sites. Variations in the frontier orbital energies and electrostatic potential distribution result from the redistribution of the electronic density across the nanotube–Ag–dopamine interface during adsorption. Properties that may be measures experimentally, such as electrical resistance, work function, and Raman enhancement, can be directly impacted by such modifications. Therefore, a clear electronic structure basis for the possible use of Ag-functionalized CNTs as dopamine sensing materials is provided by the combined effects of band-gap modulation, orbital hybridization, and charge redistribution. In comparison to the pristine nanotube and other functionalized systems, $CNTAgNH_2$ exhibits stronger localization and polarization, which further suggests increased sensitivity.

Overall, the decrease in hardness and band gap, as well as the modification of chemical potential and electrophilicity, show that Ag decoration and functional group substitution have a major impact on the stability and reactivity of drug delivery systems based on nanotubes. The Ag-decorated adsorption systems show a balanced combination of high electrophilicity, favourable chemical potential, and moderate band gap among the configurations under study, underscoring its promise for improved adsorption performance and electronic applications.

Additionally, the MEP results offer crucial information on the Ag-functionalized nanotube systems' sensing mechanism. The creation of

highly polarized adsorption sites that can enable effective charge transfer between dopamine and the nanotube surfaces is indicated by the prominent electrostatic potential gradients seen for $CNTAgNH_2$. This charge redistribution is in line with the HOMO–LUMO localization patterns, which show substantial electronic connection since the border orbitals span both the Ag-decorated CNT and the dopamine molecule. Under adsorption, such coupling is anticipated to alter the nanotube's conductivity and disturb the local electronic density. On the other hand, a smaller sensing response and less efficient electronic communication are suggested by the lower potential gradients seen for the CNTAgOH arrangement. As a result, the MEP analysis both validates the NH_2-oriented complex's greater interaction and offers a clear electronic-structure explanation for its improved sensing performance. Stronger polarization, improved charge separation, and effective orbital overlap imply that $CNTAgNH_2$ can provide a more noticeable electrical or spectroscopic signal upon dopamine adsorption, making it a suitable platform for sensitive detection applications.

Important information about the sensing behaviour of the systems under investigation is also provided by the chemical reactivity descriptors. The energy gap gradually decreases from dopamine (5.43 eV) to CNT (4.48 eV) and then to CNTAg (3.87 eV), suggesting that Ag decorating gradually improves electronic conductivity and charge-carrier mobility. This reduction in the energy gap increases the sensitivity of the nanostructure to adsorption-induced electronic disturbances by facilitating electron exchange between the adsorbate and the sensing surface. In a similar vein, the Ag-containing complexes' lower hardness values indicate more electrical flexibility and a greater propensity to experience charge redistribution during adsorption. CNTAgOH and $CNTAgNH_2$'s favourable chemical potential and comparatively strong electrophilicity further imply an improved capacity to engage in donor–acceptor interactions with dopamine. Together, these electronic properties show that adsorption is accompanied by important charge-transfer events that can alter the nanotube's structure. As a result, after dopamine adsorption, quantifiable changes in conductivity, work function, or spectroscopic response might be anticipated. The most advantageous combination of robust adsorption, improved polarization, moderate band gap, and effective charge-transfer capability among the systems under investigation is $CNTAgNH_2$, indicating its potential as a sensitive dopamine sensing platform rather than only an adsorption substrate.

3.3. Thermodynamic parameters

Complementary information about the driving forces and viability of the adsorption process is provided by the thermodynamic characteristics shown in Table S2. The thermodynamic numbers show the energetic and entropic contributions controlling complex formation, whereas adsorption energy measures the strength of the drug molecule's interaction with the nanotube surface. Adsorption is energetically advantageous and exothermic, as indicated by the negative values of ΔE and ΔH observed for all complexes, indicating that energy release occurs during the formation of the adsorbate–nanotube combination. On the other hand, the overall thermodynamic viability of adsorption under ambient conditions is reflected by the Gibbs free energy change (ΔG). A higher propensity for spontaneous complex formation is shown by the larger negative ΔG values seen for the Ag-decorated systems, underscoring the advantageous function of Ag decoration in encouraging adsorption. As the drug molecule becomes increasingly restricted on the nanotube surface during adsorption, the negative entropy changes (ΔS) seen for all systems showed a decrease in molecular flexibility. For the Ag-decorated compounds, this entropy loss is more noticeable, indicating a higher level of structural organization at the adsorption interface. As a result, the adsorption process is primarily enthalpy-driven, where the entropy penalty related to molecular confinement is outweighed by the advantageous energetic contribution. Overall, the thermodynamic study shows that Ag decoration increases the stability and spontaneous generation of the adsorption complexes through advantageous enthalpic contributions, in addition to strengthening the contact [57–59].

3.4. NCI & RDG studies

3.4.1. Dopamine

Dopamine's noncovalnet interaction (NCI) plot offers a thorough illustration of the weak intramolecular and intermolecular interactions that control its structural stability and reactivity (Fig. S4a). The colourful isosurfaces in this illustration show areas of decreased density gradient; green surfaces represent weak van der Waals contacts, blue areas represent strong attractive interactions like hydrogen bonds, and red areas reflect steric repulsion. Significant noncovalent interactions are visible in the plot surrounding the amine side chain and the hydroxyl groups of the ring, indicating their function in maintaining molecule shape and promoting interactions with biological targets. These characteristics are especially crucial for comprehending how dopamine binds in the receptor settings, where its biological activity is influenced by minute electronic and steric effects [60].

Dopamine's Reduced Density Gradient scatter plot as a function of $\text{sign}(\lambda_2)\rho$ shows discrete areas that correspond to various noncovalent interaction regimes (Fig. S4b). The RDG values range from ~0.0 to ~2.0, and the horizontal axis covers roughly −0.05 to +0.05 a.u. Strong attractive interactions, mainly related to hydrogen bonding involving the hydroxyl groups are indicated by a prominent spike in the negative $\text{sign}(\lambda_2)\rho$ region (≈ −0.035 to −0.010 a.u.) with RDG values < ~1.2. Weak van der Waals interactions are represented by a dense distribution of points with RDG < 1.0 about $\text{sign}(\lambda_2)\rho \approx -0.010$ to +0.010 a.u., which forms the distinctive green region in the NCI depiction. On the other hand, steric repulsion inside the molecular framework is reflected in the positive region (≈ +0.010 to +0.050 a.u.), which exhibits a wide spread with RDG values between ~0.5 and 1.5. The coexistence of stabilizing and destabilizing intra molecular contacts that affect dopamine's conformational behaviour is confirmed by the occurrence of a prominent low-RDG trough near $\text{sign}(\lambda_2)\rho \approx \pm 0.020$ a.u. (RDG ≈ 0.2–0.4), which further highlights discrete interaction zones [61].

3.4.2. CNT

The carbon nanotube's Noncovalent Interaction (NCI) figure shows that weak dispersive and steric interactions predominate in the extended π-conjugated framework (Fig. S5a). Red isosurfaces scattered along the inner and outer walls of the nanotube, which represent areas of intense steric repulsion resulting from the near proximity of neighbouring carbon atoms in the bent lattice, are the main characteristics of the image. The underlying symmetry and repeating bonding pattern of the nanotube structure are reflected in the periodic arrangement of these repulsive zones along the tube axis. Furthermore, weak van der Waals interactions between nearby carbon atoms can be seen as small, diffuse green isosurfaces that support the system's overall stabilization. Strong attractive interactions, such as hydrogen bonding, may not exist in this exclusively carbon-based system, as indicated by the lack of notable blue regions. Overall, the NCI analysis shows that a balance between delocalised π-π interactions within the conjugated network and steric limitations imposed by curvature governs the stability of the carbon nanotube.

The CC nanotube's reduced density gradient (RDG) analysis offers quantitative information on the type and intensity of noncovalent interactions throughout the system (Fig. S5b). The most important interaction regions are clustered below RDG = 1.0, with RDG values ranging from roughly 0.1 to 2.0 a.u. Different interaction regimes are easily distinguished by the horizontal axis, $\text{sign}(\lambda_2)\rho$, which varies from approximately −0.05 to +0.05 a.u. Blue coloured spikes are indicative of relatively weak but observable attractive interactions in the negative region (−0.05 to −0.01 a.u.), with peak density at $\text{sign}(\lambda_2)\rho \approx -0.03$ a.u. and RDG ≈ 0.8–1.2. Weak van der Waals interactions are represented by the green region near $\text{sign}(\lambda_2)\rho \approx 0$ (−0.01 to +0.01 a.u.), which

exhibits a wide distribution with RDG values between 1.0 and 1.8, representing dispersive forces inside the nanotube framework. On the other hand, red coloured spots, which indicate significant steric repulsion, dominate the positive area (+0.01 to +0.05 a.u.), with a dense concentration around sign(λ_2)ρ ≈ +0.02 to +0.04 a.u. and RDG values falling to low as ~0.2–0.6. Areas with extremely low electron density and no interaction are indicated by the abrupt spike around sign(λ_2)ρ ≈ 0 and RDG nearing 2.0. Overall, the RDG profile shows that weak dispersive interactions and steric repulsion dominate the CC nanotube, with attractive noncovalent forces contributing very little.

3.4.3. CNTAg

The Ag-doped CC nanotubes's noncovalent interaction (NCI) plot reveals a distinct spatial differentiation of interaction types brought about by the presence of silver atoms at one end of the structure (Fig. S6a). Because of the dense packing and curvature of the carbon network, steric repulsion predominates within the nanotube framework, as evidenced by the primarily red isosurfaces. On the other hand, the area surrounding the Ag atoms exhibits clear blue isosurfaces, indicating localized stability at the doped site due to attractive interactions between the silver atoms and the nearby carbon atoms. Furthermore, weak dispersive (van der Waals) interactions that support the system's overall stability are represented by diffuse green isosurfaces seen in the interfacial regions. Ag inclusion dramatically alters the interaction pattern at the interface, generating advantageous interactions while maintaining the intrinsic structural properties of the carbon nanotube, as shown by the localization of blue and green regions close to the doped end.

The Ag-doped CC nanotube's RDG figure shows a distinctive distribution of interaction regions spanning the sign(λ_2)ρ range of roughly −0.05 to +0.05 a.u., with RDG values ranging from ~0.1 up to 2.0 a.u. (Fig. S6b). Significant attractive interactions are indicated by the dense population of blue-coloured spots that dominate the negative region (−0.05 to −0.01 a.u.), with the largest concentration around sign(λ_2)ρ ≈ −0.03 a.u. and RDG values in the range of ~0.6–1.2. This area seems more populated than the pure nanotube, indicating increased interaction as a result of Ag inclusion. Green-coloured spots with RDG values between ~1.0 and 2.0 are widely scattered in the near-zero area (−0.01 to +0.01 a.u.), indicating weak van der Waals interactions at the metal–carbon contact and within the nanotube framework. Strong steric repulsion is indicated by a conspicuous cluster of red-coloured spots in the positive region (+0.01 to +0.05 a.u.), with a maximum density around sign(λ_2)ρ ≈ +0.02 to +0.04 a.u. and RDG values falling to ~0.2–0.8. Low-density non-interacting regions are represented by a steep spike at sign(λ_2)ρ ≈ 0 with RDG nearing ~2.0. Overall, the RDG profile shows that Ag doping preserves the intrinsic steric repulsion and dispersive properties of the carbon nanotube system while introducing a discernible increase in attractive interactions [62].

3.4.4. CNTOH

When dopamine's OH group is present, the noncovalent interaction (NCI) plot of the CC nanotube shows a complicated interplay of interaction types at the molecule-nanotube surface interface (Fig. 7a). Scattered red isosurfaces in the nanotube framework show that steric repulsion predominates in the tightly packed carbon network. On the other hand, strong attractive contacts, especially between the hydroxyl (OH) group and the π-electron cloud of the carbon surface, are indicated by prominent blue isosurfaces in the area where the dopamine molecule approaches the nanotube. These blue areas imply the existence of π-H type interactions or hydrogen bonding that contributes to localized stabilization. Green isosurfaces, which indicate weak van der Waals interactions that promote adsorption, are also seen surrounding the dopamine-nanotube contact region. These coloured isosurfaces' spatial distribution shows that the interaction is highly localized at the functional group location, where the OH group is crucial for anchoring the molecule to the nanotube. Weaker dispersive interactions occur throughout the rest of the structure. Overall, the NCI analysis shows that the intrinsic steric properties of the nanotube framework are superimposed atop a combination of dispersive and attractive interactions

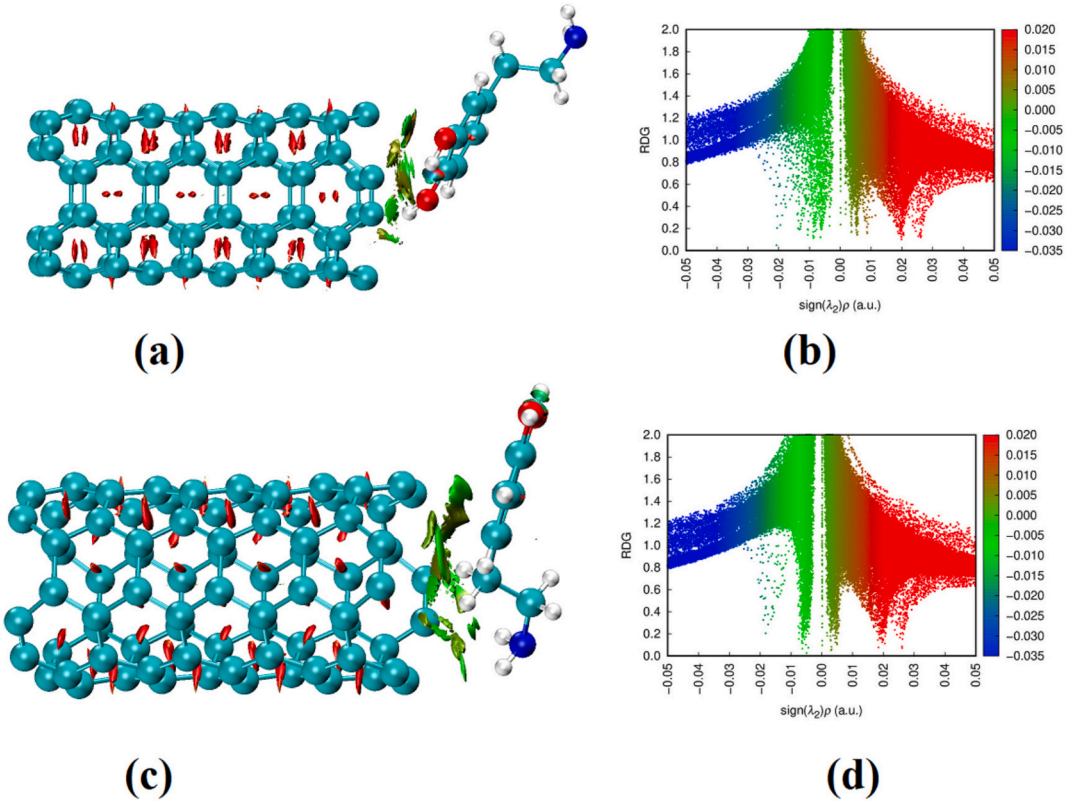

Fig. 7. CNTOH's (a) NCI (b) RDG plots; CNTNH2's (c) NCI (d) RDG plots.

that control dopamine adsorption on the CC nanotube.

With RDG values ranging from ~0.1 to 2.0 a.u., the RDG plot of the CC nanotube interacting with the OH group of dopamine displays a clearly defined distribution of noncovalent interactions across the sign (λ_2)ρ range of roughly −0.05 to +0.05 a.u (Fig. 7b). Significant attractive interactions are indicated by a dense cluster of blue-coloured spots in the negative region (−0.05 to −0.01 a.u.) with the largest concentration around sign(λ_2)ρ ≈ −0.03 a.u. and RDG values in the range of ~0.6–1.2. Strong localized contacts between the hydroxyl group and the nanotube surface are suggested by this increased density in the negative area. Green-coloured spots with RDG values between ~1.0 and 2.0 are widely dispersed in the near zero area (−0.01 to +0.01 a.u.), indicating weak van der Waals interactions that sustain the adsorption configuration. Red-coloured dots, which indicate steric repulsion, predominate in the positive area (+0.01 to +0.05 a.u.), with a high density surrounding sign(λ_2)ρ ≈ +0.02 to +0.04 a.u. and RDG values falling to ~0.2–0.8. Regions with very low electron density and no interaction are shown by a steep vertical spike at sign(λ_2)ρ ≈ 0 with RDG nearing ~2.0. Overall, the RDG profile demonstrates that a mix of dispersion and steric contributions from the carbon framework and localized attractive forces, mostly related to the OH group, control the interaction between dopamine and the nanotube.

3.4.5. $CNTNH_2$

Dopamine adsorption on the carbon nanotube surface is mostly controlled by weak, dispersive interactions with a localized contribution from the amine functionality, according to the noncovalent interaction (NCI) analysis (Fig. 7c). Significant van der Waals contacts between the aromatic moiety of dopamine and the nanotube's π-conjugated surface are shown by the extended green isosurfaces scattered along the sidewall of the nanotube, which is consistent with π-π stacking stabilization. On the other hand, the area next to the NH_2 group shows more concentrated and somewhat stronger characteristics, indicating the existence of mild attractive contacts between the amine hydrogens and the nanotube surface, most likely a mix of hydrogen bonding and electrostatic contributions. A favourable adsorption configuration is supported by the lack of noticeable red isosurfaces, which suggests low steric repulsion. Overall, the NCI profile shows that dispersion forces are the primary driver of dopamine binding, with the amine group contributing extra stability and orientational preference at the interface.

The noncovalent interactions between the carbon nanotube and dopamine with the NH_2 group oriented toward the surface are further quantified by the RDG study. Around sign(λ_2)ρ ≈ −0.01 to −0.02 a.u., the RDG scatter plot shows a prominent spike in the low-density, low-gradient region (RDG < 0.5) (Fig. 7d). This is indicative of weak but attractive interactions, compatible with hydrogen bonding and π-π contributions. Dominant van der Waals interactions across the interface are indicated by a wide array of locations centered near sign(λ_2)ρ ≈ 0.00 a.u. with RDG values extending up to ~2.0. On the other hand, the repulsive regime (sign(λ_2)ρ ≈ +0.01 to +0.04 a.u.) is mostly limited to larger RDG values (>0.8) and is quite diffuse, indicating negligible steric hindrance. While the modest skew toward negative values indicate further stability resulting from the amine group's closeness to the nanotube surface, the overall symmetric spread from −0.05 to +0.05 a.u., reveals that dispersion interactions are prominent.

3.4.6. CNTAgOH

Significant intermolecular contacts between dopamine and the Ag-decorated carbon nanotube surface are revealed by the non-covalent interaction (NCI) study of the dopamine/CNT–Ag system, especially when the hydroxyl (—OH) group of dopamine is directed toward the Ag atom (Fig. 8a). While the localized blue areas surrounding the Ag…OH interface show attractive contacts with attractive intermolecular interactions and enhanced interfacial stabilization, the green isosurfaces

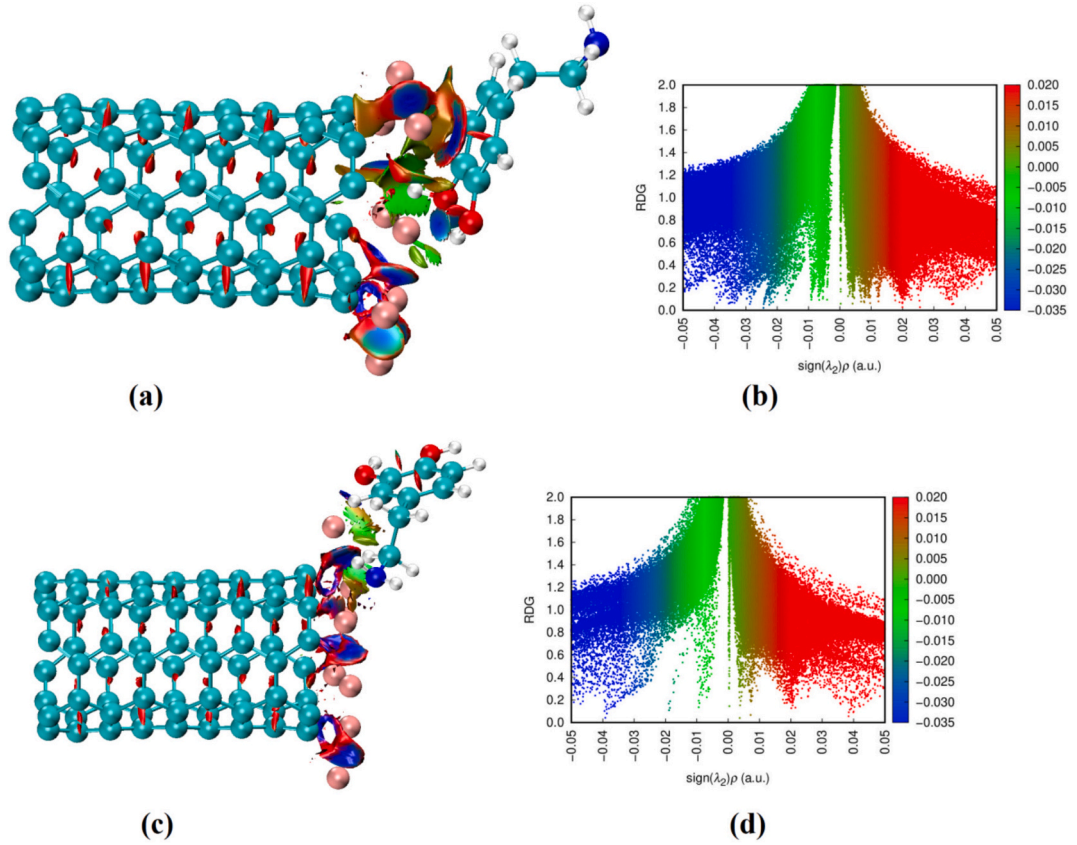

Fig. 8. CNTAgOH's (a) NCI (b) RDG plots; CNTAgNH2's (c) NCI (d) RDG plots.

seen in the NCI plot indicate dominant weak van der Waals interactions. These findings suggest that the silver atom provides a favourable adsorption site, increasing dopamine's affinity for the CNT surface via cooperative metal–molecule interactions. Additionally, the CNT's expanded π-framework stabilizes the adsorption complex by generating more π-π and dispersive interactions. Such behaviour is in line with recent research showing that the combined electrostatic, dispersive, and orbital interactions of the functionalized CNT- and graphene-based nanostructures lead to improved adsorption and sensing performance toward dopamine and other organic compounds. Ag decoration plays a crucial role in adjusting the electrical environment of CNT-based nanomaterials for biosensing and catalytic applications, as shown by the observed interaction pattern [63–65].

Strong attractive non-covalent interactions at the adsorption interface are confirmed by the reduced density gradient (RDG) study of the dopamine/CNT–Ag complex, in which the hydroxyl (–OH) group of dopamine is oriented toward the Ag atom (Fig. 8b). The RDG scatter plot's notable spike in the negative sign(λ_2)ρ area, about between −0.035 and − 0.010 a.u., is indicative of weak hydrogen-bond like interactions and attractive interactions related to the Ag···O(H) contact. Van der Waals interactions between dopamine and the carbon nanotube surface are indicated by the green-coloured region centered near sign (λ_2)ρ ≈ 0.000 a.u., while steric repulsion resulting from close-contact electron cloud overlap is represented by the red regions at positive sign(λ_2)ρ values (≈ +0.015 to +0.050 a.u.). Additionally, a comparatively stable adsorption configuration with improved electronic coupling between dopamine and the Ag-decorated CNT surface is suggested by the low RDG values (<0.5) in the attractive region. In the optimized shape, attractive interactions outweigh repulsive contributions, as evidence by the asymmetry of the RDG distribution toward negative sign(λ_2)ρ values. These results are in good agreement with recent theoretical and spectroscopic research showing that dopamine adsorption is greatly increased by silver-functionalized carbon nanostructures through metal-assisted hydroxyl binding, charge transfer, and synergistic van der Waals interactions, which improves sensing and catalytic performance [11,66,67].

3.4.7. $CNTAgNH_2$

In contrast to the pristine system, the NCI study of the Ag-doped carbon nanotube interacting with dopamine, with the hydroxyl (—OH) group facing the Ag sites, shows a different interaction pattern (Fig. 8c). Strong attractive contacts, consistent with coordination-type bonding and hydrogen bonding between the oxygen lone pairs and the Ag atoms, are shown by prominent blue isosurfaces centered at Ag—OH interface. Green isosurfaces are dispersed between the dopamine aromatic ring and the nanotube surface surrounding these areas, indicating further stabilization through van der Waals and π–surface interactions. Interestingly, tiny, localized red isosurfaces show up close to the Ag–dopamine contact zone, indicating slight steric repulsion brought on by close-range interactions. In comparison to the interactions on the undoped nanotube, the hydroxyl group functions as a primary anchoring site and contributes to a more direct and stronger binding. The increased intensity and localization of the attractive regions surrounding the Ag dopants show that metal incorporation considerably strengthens adsorption [68].

Different noncovalent interaction features are revealed throughout the sign(λ_2)ρ range from −0.05 to +0.05 a.u., by the reduced density gradient (RDG) analysis of the Ag-doped carbon nanotube interacting with the NH_2 group of dopamine (Fig. 8d). Blue-coloured spikes in the negative region (−0.05 to −0.01 a.u.) indicate strong attractive interactions. RDG values are mostly distributed between 0.6 and 1.2, suggesting the presence of moderate to strong stabilizing interactions, which are probably related to hydrogen bonding and N—H···Ag coordination. A dense concentration of green spots with RDG values up to ~2.0 around the near-zero area (−0.01 to +0.01 a.u.) indicates that weak van der Waals interactions dominate the interfacial region between the NH_2 group and the nanotube surface. The red-coloured scatter with RDG values between ~0.3 to 1.0 in the positive region (+0.01 to +0.05 a.u.) indicates spatial congestion around the Ag adsorption site and the adjacent functional group, which is indicative of steric repulsion. While weaker dispersive forces and localized steric effects collectively affect the overall interaction landscape, the symmetric distribution and intensity of spikes, especially the strong concentration near sign(λ_2)ρ ≈ −0.02 a.u., confirm that attractive interactions play a significant role in stabilizing the adsorption configuration [69].

It should be mentioned that NCI and RDG analyses, which offer qualitative and semi-quantitative data about the spatial distribution and strength of attractive, dispersive, and repulsive interactions, are the main sources of the current interpretation of the adsorption mechanism. Dopamine and the Ag-doped CNT surface exhibit enhanced attractive interactions, as shown by the observed blue NCI isosurfaces and negative sign(λ_2)ρ areas. However, these investigations do not allow for an unambiguous assessment of bond type. Therefore, rather than providing conclusive evidence of chemisorption or coordination bonding, the revealed interaction features should be viewed as proof of enhanced adsorption and advantageous intermolecular interactions. Future research would benefit from more thorough characterization using QTAIM, ELF, bond-order, or charge-partitioning techniques.

3.5. Recovery periods

The calculated recovery times at 400 K reveal substantial differences in the desorption behaviour of dopamine from pristine and Ag-doped CNT surfaces, providing important insight into the sensing and recyclability characteristics of the proposed SERS substrates (Table S3) [70,71]. The CNTOH complex, with a binding energy of −13.05 kcal mol^{-1}, exhibited ultrafast recovery times of 4.50×10^{-10}, 1.80×10^{-08}, 3.14×10^{-06} s for attempt frequencies of 3.0×10^{16}, 7.5×10^{14}, and 4.3×10^{12} Hz, respectively. Similarly, $CNTNH_2$ showed even shorter recovery times of 4.85×10^{-11}, 1.94×10^{-09}, 3.39×10^{-7}, corresponding to its relatively weaker adsorption energy of −11.28 kcal mol^{-1}. These very short desorption times indicate physisorption-dominated interactions and rapid regeneration capability of pristine CNT-based sensors. In contrast, the Ag-doped systems displayed markedly longer recovery times due to stronger dopamine adsorption. CNTAgOH, having a binding energy of −27.03 kcal mol^{-1}, showed recovery times increasing from 1.96×10^{-02} s to 1.37×10^{02} s depending on the attempt frequency, indicating moderate chemisorption and improved analyte retention on the SERS-active surface. The strongest interaction was observed for $CNTAgNH_2$, where the binding energy reached −45.25 kcal mol^{-1}, producing exceptionally long recovery times of 1.77×10^{8}, 7.06×10^{9}, and 1.23×10^{12} s. This behaviour confirms the dominant role of Ag-mediated charge transfer between dopamine NH_2 and doped CNT surface, resulting in highly stable adsorption complexes. Such enhanced adsorption is advantageous for ultrasensitive SERS detection because stronger molecule–substrate coupling increases Raman enhancement and signal stability, although excessively long recovery times may limit sensor reusability. Similar adsorption-controlled SERS enhancement mechanisms for dopamine on Ag-based nanostructures and CNT hybrid substrates have been reported in recent experimental and theoretical studies [72,73]. Adsorption strength and recovery capacity should be balanced in an ideal sensing substrate; too high adsorption results in longer recovery durations, while too weak adsorption may reduce detection sensitivity. Recovery time is therefore a crucial criterion for evaluating the usefulness of CNT-based sensing materials.

3.6. Spectral analysis

Dopamine, pure carbon nanotubes (CNTs), and Ag-doped CNT systems exhibit distinct differences in the computed density of states (DOS) spectra. A distinct gap develops around the Fermi level (0 eV), indicating

molecular-like semiconducting activity, while the DOS for the isolated dopamine molecule is highly discrete with sharp peaks centered mostly in the valence regions (−20 to −5 eV), reaching maximum intensities of ~2.0–2.2 states eV^{-1} (Fig. S7a). The pristine CNT, on the other hand, has a nearly zero DOS at the Fermi level, which is compatible with semiconducting nanotubes, and a wider, quasi-continuous DOS with distinctive van Hove singularities and peak amplitudes rising up to ~10–12 states eV^{-1} (Fig. S7b) [74].

The DOS around the Fermi level is significantly enhanced with Ag doping at one end, with new states appearing between −2 and + 2 eV and peak intensities rising to ~11–12 states eV^{-1}, indicating charge transfer and partial metallization (Fig. S7c). This result is in line with recent research that demonstrates how metal doping increases conductivity and decreases the band gap by shifting the Fermi level and adding new electronic states [75]. Quantitatively, n-type properties and increased electrical activity are reflected in the Fermi level of CNT systems, which normally resides about −4.8 eV relative to vacuum and shifts toward the conduction band upon doping [76]. Overall, there is a steady rise in DOS magnitude and continuity from discrete molecular states (dopamine) to quasi-one-dimensional band features (CNT) and finally to dopant-induced metallic states (CNTAg). This is important for charge transport and sensing applications.

When the molecule interacts through distinct functional groups (—OH vs —NH_2) and when Ag doping is present the DOS spectra of CNT-dopamine complexes clearly demonstrate configuration-dependent electronic changes. The valence band region (−18 to −8 eV) displays several peaks with intensities up to ~10–11 states eV^{-1}, while the DOS displays a semiconducting profile with a prominent gap around the Fermi level (0 eV) of roughly 1.5–2.0 eV for the pristine CNT-dopamine system with the hydroxyl (—OH) group oriented toward the nanotube (Fig. S8a). By contrast, the —NH_2 configuration results in a minor shift of spectral weight toward the Fermi level and a somewhat greater DOS intensity around the conduction region (+2 to +10 eV), reaching ~11 states eV^{-1}, suggesting stronger electronic coupling and potential charge transfer (Fig. S8b). These variations align with first-principles research demonstrating that dopamine can change the electrical structure of CNTs by donating electrons without necessarily creating deep mid-gap states [77].

The DOS spectra undergo dramatic changes upon Ag doping; for the CNTAg with dopamine (-OH) configuration, peak intensities in the valence region remain high (~11–12 states eV^{-1}), while the band gap narrows to ~1.0 eV and new states appear near −2 to 0 eV (Fig. S8c). The impacts is much more noticeable in the —NH_2 configuration, where increased states between −1 and +3 eV and a nearly continuous DOS across the Fermi level show quasi-metallic behaviour and stronger hybridization between Ag, CNT, and dopamine orbitals (Fig. S8d). According to recent reports, CNT-based dopamine systems exhibit charge transfer interactions and adsorption energies on the order of ~0.6–0.75 eV, which are sufficient to perturb the electronic structure while maintaining structural stability. This enhancement in DOS near the Fermi level suggests improved conductivity and sensing capability [77]. Overall, the findings show that metal doping and molecule orientation both affect the band gap (from ~1.0 eV to ~1.0 eV or less) and DOS magnitude (from ~6 up to ~12 states eV^{-1}), underscoring their crucial role in fine-tuning CNT-based nanosensors for neurotransmitter detection.

The theoretically predicted frequencies of dopamine are: 3720, 3665, 1202, (OH), 3472, 3384 (NH2), 3096, 1655, 1302, 1164, 782 (phenyl ring), 2977, 2934, 1462, 1364 (CH2), 1091 (CN), 1015 cm^{-1} (CC) in Raman spectrum and at 3723, 3659, 1333, 1199 (OH), 3389, 1633 (NH_2), 3096, 3080, 1533, 1485, 1165, 1119, 855, 786, 629 (phenyl ring), 3007, 2955, 2928, 1364, 1085, 966, 745 (CH2), 1320 (CO), 1017 cm^{-1} (CC) in the IR spectrum (Fig. S9) [78,79].

The enhancement factor (EF in %) was calculated using the formula $EF = (I_{complex}\text{-}I_{dopamine})/I_{dopamine}$ (where I represents Raman intensity values) and given in brackets in the following discussion [71,80]. The modes appear at 3635 (1516%), 3586 (1699%) (OH), 1651 (1953%), 779 (2564%) (phenyl ring) in CNTOH (Fig. S10a); 3465 (305%), 3375 (434%) (NH_2), 2949 (707%) (CH_2), 785 (1952%) (phenyl ring) for $CNTNH_2$ (Fig. S10b); 3515 (177%), 3463 (303%) (OH), 1083 (42089%) (CN), 945 (59689%), 896 (48872%), 812 (12449%) (phenyl ring) in CNTAgOH (Fig. S10c); 3714 (127%), 3616 (171%) (OH), 3475 (310%), 3399 (125%), 938 (NH_2), 3059 (47%), 791(2928%) (phenyl ring), 2974 (344%) (CH_2) for $CNTAgNH_2$ (Fig. S10d) in the theoretical Raman spectrum. It should be noted that the finite nanotube cluster model adopted in this work is mainly capable of describing the chemical enhancement contribution to SERS, arising from charge-transfer interactions between dopamine and the nanotube surface. As shown in Figs. 10a–10d, several vibrational modes display enhanced Raman intensities upon adsorption, accompanied by shifts relative to the corresponding modes of isolated dopamine. These spectral changes indicate alterations in molecular polarizability and electronic structure caused by adsorbate–substrate interactions [60,81,82].

The dopamine/CNT and dopamine/Ag-CNT complexes' adsorption-induced vibrational frequency shifts offer important insights into molecule–substrate interactions that could affect Raman spectrum. However, it should be noted that SERS enhancement factors, Raman activities, polarizability derivatives, plasmonic responses, and electromagnetic field enhancements are not specifically assessed in this study. Therefore, rather than being direct proof of SERS performance, the computed frequency shifts should be viewed as markers of spectrum disturbances caused by adsorption and possible chemical contributions to SERS. Although specific Raman and optical-response calculations would be necessary to establish quantitative SERS enhancement, the stronger adsorption affinity and altered vibrational characteristics observed for the Ag-doped CNT systems suggest that these materials may serve as promising candidates for future SERS substrate development.

These modes appear at 3638, 3584 (OH), 1636 (NH_2), 3083, 1521, 1476, 1150, 849, (phenyl ring), 3008, 2957, 962 (CH2), 1299 (CO), 1012 (CC) in CNTOH (Fig. S11a); 3722, 3659, 1198 (OH), 3458, 3373, 1636, 1050 (NH_2), 3071, 1530, 1476, 1160, 869, 786 (phenyl ring), 3008, 2948, 1294, 962, (CH_2) for $CNTNH_2$ (Fig. S11b); 3520, 3462, 1168, 639 (OH), 3003, 2953, 1274, 742 (CH_2), 1649 (NH_2), 894 (phenyl ring) in CNTAgOH (Fig. S11c); 3714, 3613 (OH), 3474, 3395, 1631, 1269 (NH_2), 3096, 734 (phenyl ring), 3024, 2991, 2944, 941 (CH_2) for $CNTAgNH_2$ (Fig. S11d) in the theoretical IR spectrum.

The calculated vibrational spectra clearly demonstrate that adsorption of dopamine on CNT and Ag-doped CNT substrates induces significant shifts in the OH and NH_2 stretching modes, confirming strong interfacial interactions relevant to the SERS enhancement mechanism. For isolated dopamine, the OH stretching vibrations appeared at 3720, 3665 cm − 1 in Raman and 3723, 3659 cm^{-1} in IR spectra, while the NH_2 stretching modes were observed near 3472–3384 cm^{-1} (Raman) and 3389 cm^{-1} (IR). Upon interaction with pristine CNTs, these bands shifted to lower frequencies, particularly in CNTOH where the OH modes moved to 3635 and 3586 cm^{-1}, indicating hydrogen-bonding and charge-transfer interactions between the catechol hydroxyl groups and the nanotube surface. Similarly in $CNTNH_2$, the NH_2 stretching vibration shifted to 3375 cm^{-1}, suggesting adsorption through the amine functionality. More pronounced spectral perturbations were observed for Ag-doped CNT systems, where CNTAgOH exhibited OH vibrations at 3515 and 3463 cm^{-1}, and $CNTAgNH_2$ showed NH_2 bands at 3475 and 3399 cm^{-1}. The larger red shifts in the Ag-containing complexes indicate stronger adsorption and enhanced electronic coupling arising from Ag-mediated charge transfer, which is known to contribute substantially to the chemical enhancement component of SERS. In addition, shifts in the phenyl ring and CH_2 vibrational modes further support modification of the dopamine electronic environment upon adsorption. These results suggest that dopamine preferentially interacts with Ag-doped CNT substrates through both hydroxyl and amine groups, leading to increased molecular polarizability and stronger Raman enhancement, consistent with current understanding of molecule–metal interfacial

interactions in SERS-active nanostructures [83–86].

4. Conclusion

This DFT study demonstrates that Ag doping significantly improves the adsorption and sensing performance of carbon nanotubes toward dopamine. Pristine CNTs interact mainly through weak physisorption, while Ag-doped CNTs show stronger binding due to enhanced charge transfer, electrostatic polarization, and metal-molecule coordination. The $CNTAgNH_2$ complex was identified as the most stable and strongly interacting system, with the most favourable adsorption and thermodynamic parameters. NCI and RDG analyses confirmed that van der Waals forces, hydrogen bonding, and Ag-assisted attractive interactions collectively stabilize the adsorbed dopamine molecule. DOS and FMO results further showed that Ag doping improves electronic conductivity and facilitates charge-transfer pathways. The enhanced adsorption affinity and adsorption-induced vibrational perturbations observed for Ag-doped CNTs suggest their potential relevance as candidate materials for dopamine sensing and motivate future investigations involving explicit Raman and SERS calculations.

Declaration of competing interest

The authors declare that they have no known competing financial interests or personal relationships that could have appeared to influence the work reported in this paper.

Acknowledgement

Princess Nourah Bint Abdulrahman University Researchers Supporting Project number (PNURSP2026R13), Princess Nourah Bint Abdulrahman University, Riyadh, Saudi Arabia. GJ express his appreciation to CIS-Laboratory, Pondicherry univeristy.

Appendix A. Supplementary data

Supplementary data to this article can be found online at https://doi.org/10.1016/j.saa.2026.128311.

Data availability

Data will be made available on request.

References

[1] A.K.M.R. Reddy, A. Darwiche, M.V. Reddy, K. Zaghib, Review on the advancements in carbon nanotubes: synthesis, purification, and multifaced applications, Batteries 11 (2025) 71, https://doi.org/10.3390/batteries11020071.
[2] M. Yoon, G.D. Samolyuk, K. Li, J.A. Hayne, T. Aytug, Improved Electrical Conductivity Of Copper And Nitrogen Functionalized Carbon Nanotubes, doi:10.48550/arXiv.2408.02884.
[3] S. Rezaie, D.M.J. Smeulders, A. Luna-Triguero, Enhanced hydrogen storage in gold-doped carbon nanotubes: a first principles study, Chem. Eng. J. 476 (2023) 146525, https://doi.org/10.1016/j.cej.2023.146525.
[4] M. Singla, D. Sharma, N. Jaggi, Effect of transition metal (Cu and Pt) doping /co-doping on hydrogen gas sensing capability of graphene: a DFT study, Int. J. Hydrog. Energy 46 (2021) 16188–16201, https://doi.org/10.1016/j.ijhydene.2021.02.004.
[5] R. Verma, N. Jaggi, Ability of transition metal and hetero atoms co-doped SWCNTs for hydrogen adsorption: a DFT study, J. Phys. Chem. Solids 194 (2024) 112244, https://doi.org/10.1016/j.jpcs.2024.112244.
[6] F.N. Ajeel, K.H. Bardan, S.H. Kareem, A.M. Khudhair, Pd doped carbon nanotubes as a drug carrier for gemcitabine anticancer drug: DFT studies, Chem. Phys. Impact 7 (2023) 100298, https://doi.org/10.1016/j.chphi.2023.100298.
[7] M. Rezazade, S. Ketabi, M. Qomi, Effect of functionalization on the adsorption performance of carbon nanotube as a drug delivery system for imatinib: molecular simulation study, BMC Chem. 18 (2024) 85, https://doi.org/10.1186/s13065-024-01197-0.
[8] U. Hani, B. Huwaimel, A.M. Alsubaiyel, S.M. Alshahrani, F. Alshammari, J. Alanazi, M. Alanazi, T.N. Alharby, DFT study of carboplatin encapsulation interactions with carboxylated carbon nanotubes and conjugated to folic acid for targeted nano delivery systems, Alex. Eng. J. 71 (2023) 501–520, https://doi.org/10.1016/j.aej.2023.03.068.
[9] M.U. Khan, I. Jabeen, A. Althagafi, M.U. Farooq, M. Harb, B. Arkook, DFT and molecular docking study of HA-conjugated SWCNTs for CD_{44}-targeted delivery of platinum-based chemotherapeutics, Pharmaceuticals (Basel) 18 (2025) 805, https://doi.org/10.3390/ph18060805.
[10] A.M. Mija, T. Debnath, Interaction of carbon nanotube with anticancer drugs busulfan and mercaptopurine: a DFT study, Comp. Theor. Chem. 1230 (2023) 114356, https://doi.org/10.1016/j.comptc.2023.114356.
[11] M. Kim, Y.S. Choi, D.H. Jeong, SERS detection of dopamine using metal-chelated ag nanoshell, RSC Adv. 14 (2024) 14214–14220, https://doi.org/10.1039/d4ra00476k.
[12] S. Duan, G. Tian, Y. Luo, Theoretical and computational methods for tip- and surface-enhanced Raman scattering, Chem. Soc. Rev. 53 (2024) 5083–5117, https://doi.org/10.1039/D3CS01070H.
[13] S.L. Luo, T.M. Swager, Chemiresistive sensing with functionalized carbon nanotubes, Nat. Rev. Methods Primers 3 (2023) 73, https://doi.org/10.1038/s43586-023-00255-6.
[14] A. Hariharan, R. Kurnoothala, S.K. Chinthakayala, K.C. Vishnubhatla, P. Vadlamudi, SERS of dopamine: computational and experimental studies, Spectrochim. Acta 260 (2021) 119962, https://doi.org/10.1016/j.saa.2021.119962.
[15] H. Cheng, H. Qiu, Z. Zhu, M. Li, Z. Shi, Investigation of the electrochemical behaviour of dopamine at electrodes modified with ferrocene-filled double-walled carbon nanotubes, Electrochim. Acta 63 (2012) 83–88, https://doi.org/10.1016/j.electacta2011.12.083.
[16] H. Kim, G. Kim, Adsorption properties of dopamine derivatives using carbon nanotubes: a first principles study, Appl. Surf. Sci. 501 (2020) 144249, https://doi.org/10.1016/j.apsusc.2019.144249.
[17] S.H. Chen, D.R. Bell, B. Luan, Understanding interactions between biomolecules and two-dimensional nanomaterials using *in silico* microscopes, Adv. Drug Deliv. Rev. 186 (2022) 114336, https://doi.org/10.1016/j.addr.2022.114336.
[18] V. Ball, Polydopamine nanomaterials: recent advances in synthesis methods and applications, Front. Bioeng. Biotechnol. 6 (2018) 109, https://doi.org/10.3389/fbioe.2018.00109.
[19] A. Roychoudhury, S. Basu, S.K. Jha, Dopamine biosensor based on surface functionalized nanostructured nickel oxide platform, Biosens. Bioelectron. 84 (2016) 72–81, https://doi.org/10.1016/j.bios.2015.11.061.
[20] Gaussian 16, Revision A.03, M.J. Frisch, G.W. Trucks, H.B. Schlegel, G.E. Scuseria, M.A. Robb, J.R. Cheeseman, G. Scalmani, V. Barone, G.A. Petersson, H. Nakatsuji, X. Li, M. Caricato, A.V. Marenich, J. Bloino, B.G. Janesko, R. Gomperts, B. Mennucci, H.P. Hratchian, J.V. Ortiz, A.F. Izmaylov, J.L. Sonnenberg, D. Williams-Young, F. Ding, F. Lipparini, F. Egidi, J. Goings, B. Peng, A. Petrone, T. Henderson, D. Ranasinghe, V.G. Zakrzewski, J. Gao, N. Rega, G. Zheng, W. Liang, M. Hada, M. Ehara, K. Toyota, R. Fukuda, J. Hasegawa, M. Ishida, T. Nakajima, Y. Honda, O. Kitao, H. Nakai, T. Vreven, K. Throssell, J.A. Montgomery Jr., J.E. Peralta, F. Ogliaro, M.J. Bearpark, J.J. Heyd, E.N. Brothers, K.N. Kudin, V.N. Staroverov, T.A. Keith, R. Kobayashi, J. Normand, K. Raghavachari, A.P. Rendell, J.C. Burant, S.S. Iyengar, J. Tomasi, M. Cossi, J.M. Millam, M. Klene, C. Adamo, R. Cammi, J.W. Ochterski, R.L. Martin, K. Morokuma, O. Farkas, J.B. Foresman, D.J. Fox, Gaussian, Inc., Wallingford CT, 2016.
[21] R. Dennington, T. Keith, J. Millam, Gaussview, Version 5, Semichem Inc., Shawnee Mission, KS, 2009.
[22] T. Lu, F. Chen, Multiwfn: a multifunctional wavefunction analyzer, J. Comput. Chem. 33 (2012) 580–592, https://doi.org/10.1002/jcc.22885.
[23] W. Humphrey, A. Dalke, K. Schulten, VMD: visual molecular dynamics, J. Mol. Graph. 13 (1996) 33, https://doi.org/10.1016/0263-7855(96)00018-5.
[24] N. Fatima, Sajeela, K. Mustafa, F.T. Amnber, M. Iqbal, A. Rafique, J. Nawaz, N. Faatima, N. Ikram, Designing smarter hole transport materials: a review of theory-driven molecular strategies for next generation solar cells, Sarcouncil J. Appl. Sci. 5 (2025) 52–66, https://doi.org/10.5281/zendo.16932671.
[25] J. Chai, M. Head-Gordon, Long-range corrected hybrid density functionals with damped atom-atom dispersion corrections, Phys. Chem. Chem. Phys. 10 (2008) 6615–6620, https://doi.org/10.1039/B810189B.
[26] N. Yuksel, A. Kose, M.F. Fellah, Pd, Ag and Rh doped (8,0) single-walled carbon nanotubes (SWCNTs): a DFT study on furan adsorption and detection, Surf. Sci. 715 (2022) 121939, https://doi.org/10.1016/j.susc.2021.121939.
[27] S. Demir, M.F. Fellah, Carbon nanotubes doped with Ni, Pd and Pt: a density functional theory study of adsorption and sensing NO, Surf. Sci. 701 (2020) 121689, https://doi.org/10.1016/j.susc.2020.121689.
[28] A.I. Alrawashdeh, J.B. Lagowski, The role of the solvent and size of the nanotube in the non-covalent dispersion of carbon nanotubes with short organic oligomers – a DFT study, RSC Adv. 8 (2018) 30520–30529, https://doi.org/10.1039/C8RA02460J.
[29] Y. Yang, M.N. Weaver, K.M. Merz Jr., Assessment of the "6-31+G**+LANL2DZ" mixed basis set coupled with density functional theory methods and the effective core potential: predictions of heats of formation and ionization potentials for the first-row transition-metal complexes, J. Phys. Chem. A 113 (2009) 9843–9851, https://doi.org/10.1021/jp807643p.
[30] A. Siiskonen, A. Priimagi, Benchmarking DFT methods with small basis sets for the calculation of halogen-bond strengths, J. Mol. Model. 23 (2017) 50, https://doi.org/10.1007/s00894-017-3212-4.
[31] S.M. Monavari, F. Marsusi, N. Memarian, M. Qasemnazhand, Carbon nanotubes and nanobelts as potential materials for biosensor, Sci. Rep. 13 (2023) 3118, https://doi.org/10.1038/s41598-023-29862-9.

[32] M. Zhang, S. Inoue, Y. Matsumura, Mechanism simulation of polar and nonpolar organic solvent vapor adsorption on a multiwall carbon nanotubes paper gas sensor, RSC Adv. 14 (2024) 24985–24991, https://doi.org/10.1039/D4RA04474F.
[33] B. Li, C. Mi, Atomistic insights on the adsorption of long-chain undecane molecules on carbon nanotubes: roles of chirality and surface hydroxylation, Diamond Rel. Mater. 133 (2023) 109706, https://doi.org/10.1016/j.diamond.2023.109706.
[34] F. Weigend, R. Ahlrichs, Balanced basis sets of split valence, triple zeta valence and quadruple zeta valence quality for H to Rn: design and assessment of accuracy, Phys. Chem. Chem. Phys. 7 (2005) 3297–3305, https://doi.org/10.1039/B508541A.
[35] D. Andrae, U. Haubermann, M. Dolg, H. Stoll, H. Preb, Energy-adjusted ab initio pseudopotentials for the second and third row transition elements, Theoret. Chim. Acta 77 (1990) 123–141, https://doi.org/10.1007/BF01114537.
[36] C. Bannwarth, E. Caldeweyher, S. Ehlert, A. Hansen, P. Pracht, J. Seibert, S. Spicher, S. Grimme, Extended tight-binding quantum chemistry methods, WIREs Comput. Mol. Sci. 11 (2021) e1493, https://doi.org/10.1002/wcms.1493.
[37] J.S. Al-Otaibi, Y.S. Mary, M.C. Gamberini, Unlocking the potential of lamotrigine in nanotubes: DFT, MD simulations in different solvents, sensing properties and drug enhancer, Surf. Sci. 761 (2025) 122789, https://doi.org/10.1016/j.susc.2025.122789.
[38] Z.H. Al-Sawaff, S.S. Dalgic, F. Kandemirli, M. Monajjemi, F. Mollaamin, DFT study adsorption of hydroxychloroquine for treatment of COVID-19 by SiC nanotube and Al, Si doping on carbon nanotube surface: a drug delivery simulation, Russ. J. Phys. Chem. 96 (2022) 2953–2966, https://doi.org/10.1134/s003602442213026X.
[39] B.I. Kharisov, O.V. Kharissova, U.O. Mendez, I.G. De La Fuente, Decoration of carbon nanotubes with metal nanoparticles: recent trends, synthesis and reactivity in inorganic, meta-organic and nano-metal, Chemistry 46 (2016) 55–76, https://doi.org/10.1080/15533174.2014.900635.
[40] M.V. Kharlamova, M. Paukov, M.G. Burdanova, Nanotube functionalization; investigation, methods and demonstrated applications, Materials 15 (2022) 5386, https://doi.org/10.3390/ma15155386.
[41] M.S. Ribeiro, A.L. Pascoini, W.G. Knupp, I. Camps, Effects of surface functionalization on the electronic and structural properties of carbon nanotubes: a computational approach, Appl. Surf. Sci. 426 (2017) 781–787, https://doi.org/10.1016/apsusc.2017.07.162.
[42] J. Wang, K.-S. Liao, D. Fruchtl, Y. Tian, A. Gilchrist, N.J. Alley, E. Anderoli, B. Aitchison, A.G. Nasibulin, H.J. Byrne, E.I. Kauppinen, L. Zhang, W.J. Blau, S. A. Curran, Nonlinear optical properties of carbon nanotube hybrids in polymer dispersion, Mater. Chem. Phys. 133 (2012) 992–997, https://doi.org/10.1016/j.matchemphys.2012.02.003.
[43] A. Abbasi, R.M. Rzayev, A.A. Niyazova, D. Sur, S. Ballal, N.K. Karimova, A. E. Suleymanova, Enhanced adsorption and biosensing performance of adenine ($C_5H_5N_5$) and guanine ($C_5H_5N_5O$) nucleobases on the novel ZnO-MoSe2 nanosheets: a theoretical study, Mater. Chem. Phys. 337 (2025) 130559, https://doi.org/10.1016/j.matchemphys.2025.130559.
[44] K. Fukui, Role of frontier orbitals in chemical reactions, Science 218 (1982) 747–754, https://doi.org/10.1126/science.218.4574.747.
[45] P. Politzer, J.S. Murray, The fundamental nature and role of the electrostatic potential in atoms and molecules, Theor. Chem. Accounts 108 (2002) 134–142, https://doi.org/10.1007/s00214-002-0363-9.
[46] J.S. Al-Otaibi, F.S. Alamro, A.H. Amugrin, Y.S. Mary, G. Jhaa, M.S. Roxy, M. C. Gamberini, Computational and spectroscopic insights into 2-(3-methylureido) acetic acid (MUA) adsorption and sensing on coinage bimetallic nanoclusters, Chem. Phys. 604 (2026) 113100, https://doi.org/10.1016/j.chemphys.2026.113100.
[47] Z. Ullah, F. Sattar, H.J. Kim, S. Jang, Y.S. Mary, X. Zhan, H.W. Kwon, Computational study of Pd-Cd bimetallic crystals: spectroscopic properties, hirshfeld surface analysis, non-covalent interaction and sensor activity, J. Mol. Liq. 365 (2022) 120111, https://doi.org/10.1016/j.molliq.2022.120111.
[48] J.S. Al-Otaibi, Y.S. Mary, Y.S. Mary, Z. Ullah, H.W. Kwon, Adsorption behaviour and solvent effects of an adamantine-triazole derivative on metal clusters – DFT simulation studies, J. Mol. Liq. 345 (2022) 118242, https://doi.org/10.1016/j.molliq.2021.118242.
[49] A.H. Almuqrin, J.S. Al-Otaibi, Y.S. Mary, Y.S. Mary, DFT computational study towards investigating psychotropic drugs, promazine and trifuloperazine adsorption on graphene, fullerene and carbon cyclic ring nanoclusters, Spectrochim. Acta 246 (2021) 119012, https://doi.org/10.1016/j.saa.2020.119012.
[50] J.S. Al-Otaibi, Y.S. Mary, Y.S. Mary, N. Acharjee, Z. Ullah, DFT, solvation effects, reactivity and SERS analysis on structural, optical, and vibrational properties of a biomolecule pyrimidine derivative adsorbed on metal clusters of Ag/Au/Cu, J. Indian Chem. Soc. 99 (2022) 100753, https://doi.org/10.1016/j.jics.2022.100753.
[51] H.M. Ngo, U. Pal, Y.S. Kang, K.M. Ok, DFT-based study for the enhancement of CO_2 adsorption on metal-doped nitrogen-enriched polytriazines, ACS Omega 8 (2023) 8876–8884, https://doi.org/10.1021/acsomega.3c00395.
[52] E.C.R. Lopez, Transition metal dopants modulate the band gap and electronic structure of corrugated graphitic carbon nitride, Next Mater. 8 (2025) 100550, https://doi.org/10.1016/j.nxmate.2025.100550.
[53] R.G. Parr, R.G. Pearson, Absolute hardness: companion parameter to absolute electronegativity, J. Am. Chem. Soc. 105 (1983) 7512–7516, https://doi.org/10.1021/ja00364a005.
[54] P. Geerlings, F. De Proft, W. Langenaeker, Conceptual density functional theory, Chem. Rev. 103 (2003) 1793–1874, https://doi.org/10.1021/cr990029p.
[55] J. Qi, P. Zhang, T. Zhang, R. Zhang, Q. Zhang, J. Wang, M. Zong, Y. Gong, X. Liu, X. Wu, B. Li, Metal-doped carbon dots for biomedical applications: from design to implementation, Heliyon 11 (2024) e32133, https://doi.org/10.1016/j.heliyon.2024.e32133.
[56] P.T. Be, N.T. Hang, L.V. Khu, H.V. Hung, B.C. Trinh, V.M. Tan, N.N. Ha, N.T.T. Ha, Study on the adsorption of 2,4-dichlorophenoxyacetic acid on silver doped carbon nanotube using tight-binding quantum chemical method, Comput. Theor. Chem. 1234 (2024) 114517, https://doi.org/10.1016/j.comptc.2024.114517.
[57] N. Patrignani, J. Juan, O. Nagel, W. Reimers, R. Luna, P.V. Jasen, The adsorption of CO and NO on (8,0) SWCNT decorated with transition metals: a DFT study as a possible gas sensor, Powder Technol. 438 (2024) 119691, https://doi.org/10.1016/j.powtec.2024.119691.
[58] Y.S. Itas, M.U. Khandaker, M. Mohmoud, Evaluating the CO2 capture potential of MgO sheets: a DFT study on the effects of vacancy and Ni doping for assessing environmental sustainability, RSC Adv. 15 (2025) 3047–3059, https://doi.org/10.1039/D4RA08592B.
[59] C.P. Bhat, P. Suryawanshi, A. Guneja, D. Bandyopadhyay, Unveiling the adsorption and electronic interactions of drug on 2D graphsene: insights from DFT and machine learning approaches, Mater. Ad. 7 (2026) 2803–2812, https://doi.org/10.1039/D5MA01519G.
[60] J.S. Al-Otaibi, Y.S. Mary, N. Acharjee, R.K. Trivedi, B. Chakraborty, M.S. Roxy, DFT investigations of therapeutic competence of B_3O_3 as an efficient drug delivery agent for phosphonoacetic acid (PAA) antiviral drug, Comput. Theor. Chem. 1252 (2025) 115406, https://doi.org/10.1016/j.comptc.2025.115406.
[61] J.S. Al-Otaibi, Y.S. Mary, C. Gend, B. Chakraborty, Unlocking on the effect of gold cluster with pregabalin, a bioactive molecule: solvation, SERS and reactivity analysis, J. Indian Chem. Soc. 102 (2025) 101853, https://doi.org/10.1016/j.jics.2025.101853.
[62] J.S. Al-Otaibi, Y.S. Mary, A. Saral, M.C. Gamberini, SERS sensing of the biomolecule of palbociclib (PCB) adsorbed on Au_3 cluster: DFT, reactivity, docking and MD simulations, Nano-Struct. Nano-Object 45 (2026) 101597, https://doi.org/10.1016/j.nanoso.2025.101597.
[63] D.G. Chandran, L. Muruganandam, R. Biswas, A review on adsorption of heavy metals from wastewater using carbon nanotube and graphene-based nanomaterials, Environ. Sci. Pollut. Res. 30 (2023) 110010–110046, https://doi.org/10.1007/s11356-023-30192-6.
[64] D.R. Rout, H.M. Jena, O. Baigenzhenov, A. Hosseini-Bandegharaei, Graphene-based materials for effective adsorption of organic and inorganic pollutants; a critical and comprehensive review, Sci. Total Enviorn. 863 (2023) 160871, https://doi.org/10.1016/j.scitotenv.2022.160871.
[65] M. Amft, S. Lebegue, O. Eriksson, N.V. Skorodumova, Adsorption of Cu, Ag, And Au atoms on graphene including van der Waals interactions, J. Phys. Condens. Matter 23 (2011) 395001, https://doi.org/10.1088/0953-8984/23/39/395001.
[66] M. Khnifira, W. Boumya, J. Attarki, A. Mahsoune, M. Abdennouri, M. Sadiq, S. Kaya, N. Barka, Adsorption characteristics of dopamine by activated carbon: experimental and theoretical approach, J. Mol. Struct. 1278 (2023) 134964, https://doi.org/10.1016/j.molstruc.2023.134964.
[67] V. Vetrivelan, S. Sakthivel, S. Muthu, A.A. Al-Saadi, Non-covalent interaction, adsorption characteristics and solvent effect of procainamide anti-arrythmias drug on silver and gold loaded silica surfaces: SERS spectroscopy, density functional theory and molecular docking investigations, RSC Adv. 13 (2023) 9539–95554, https://doi.org/10.1039/D3RA00514C.
[68] J.S. Al-Otaibi, Y.S. Mary, V. Baiju, K. Jalaja, M.C. Gamberini, Adsorption and sensing of vildagliptin on coinage metal nanoclusters: DFT, MD and spectroscopic insights, Comput. Theor. Chem. 1256 (2026) 115640, https://doi.org/10.1016/j.comptc.2025.115640.
[69] J.S. Al-Otaibi, Y.S. Mary, J.N.C. Mishma, B. Gayathri, K.S. Resmi, M.C. Gamberini, Computational insights into quetiapine adsorption on coinage metal nanoclusters: mechanistic basis for sensing and nanomedicine, Chem. Pap. (2025), https://doi.org/10.1007/s11696-025-04571-x.
[70] J.S. Al-Otaibi, F.S. Alamro, A.H. Almugrin, Y.S. Mary, A. Mondal, N. Acahrjee, M. C. Gamberini, Adsorption and electronic interactions of glycine on Al12N12 & B12N12 nanocages: a DFT study, J. Mol. Liq. 447 (2026) 129373, https://doi.org/10.1016/j.molliq.2026.129373.
[71] J.S. Al-Otaibi, Y.S. Mary, M. Ismoilov, G. Jhaa, M.C. Gamberini, Density functional theory investigations of hydroxyzine adsorption on silver clusters: implications for SERS-based sensing and interfacial stability, J. Mol. Liq. 451 (2026) 129496, https://doi.org/10.1016/j.molliq.2026.129496.
[72] M. Kim, V.S. Choi, D.H. Jeong, SERS detection of dopamine using metal-chelated ag nanoshell, RSC Adv. 14 (2024) 14214–14220, https://doi.org/10.1039/D4RA00746K.
[73] Q. Jia, B.J. Venton, K.H. DuBay, Structure and dynamics of adsorbed dopamine on solvated carbon nanotubes and in a CNT groove, Molecules 27 (2022) 3768, https://doi.org/10.3390/molecules27123768.
[74] E. Faizabadi, Single Wall carbon nanotubes in the presence of vacancies and related energy gaps, in: Electronic Properties Of Carbon Nanotubes, InTech, 2011, https://doi.org/10.5772/22654.
[75] R. Miao, Y. Liang, R. Wen, Y. Wang, Q. Shao, Theoretical and experimental investigations of carbon nanotube-gold interface conductivity through nitrogen doping, Nanoscale 16 (2024) 249–261, https://doi.org/10.1039/D3NR04588A.
[76] S.M. Kim, K.K. Kim, D.L. Duong, Y. Hirana, Y. Tanaka, Y. Niidome, N. Nakashima, J. Kong, Y.H. Lee, Spectroscopic determination of the electrochemical potentials of n-type doped carbon nanotubes, J. Phys. C 116 (2012) 5444–5449, https://doi.org/10.1021/jp211583t.
[77] R. Zhang, M. Zhu, T. Tian, H. Yin, T. Zhang, J. Liu, K. Dong, X. Li, B. Zhao, Y. Su, Fermi level regulation of single-walled carbon nanotubes by metal chloride doping for enhanced NO_2 sensing performance, Diam. Relat. Mater. 151 (2025) 111777, https://doi.org/10.1016/j.diamond.2024.111777.

[78] N.P.G. Roeges, A Guide to the Complete Interpretation of Infrared Spectra of Organic Structures, John Wiley and Sons Inc., NY, New York, 1994.
[79] K.B. Benzon, Y.S. Mary, H.T. Varghese, C.Y. Panicker, S. Armakovic, S. J. Armakovic, K. Pradhan, A.K. Nanda, C. Van Alsenoy, Spectroscopic, DFT, molecular dynamics and molecular docking study of 1-butyl-2-(4-hydroxyphenyl)-4,5-dimethyl-imidazole 3- oxide, J. Mol. Struct. 1134 (2017) 330–344, https://doi.org/10.1016/j.molstruc.2016.12.100.
[80] V. Sharma, N.N. Som, S.B. Pillai, P.K. Jha, Utilization of doped GQDs for ultrasensitive detection of catastrophic melamine: a new SERS platform, Spectrochim. Acta 224 (2020) 117352, https://doi.org/10.1016/j.saa.2019.117352.
[81] J.S. Al-Otaibi, Y.S. Mary, M. Kratky, J. Vinsova, M.C. Gamberini, SERS, docking and MD simulations of 2-methylene-4-oxo-4[(3,4,5-trichlorophenyl)amino]butanoic acid (MTB): experimental and DFT modelling, Surf. Sci. 764 (2026) 122857, https://doi.org/10.1016/j.susc.2025.122857.
[82] J.S. Al-Otaibi, Y.S. Mary, M.C. Gamberini, Exploring the potential of AuSb and Ca/K/Mg/−decorated nanocages as a promising tool for adsorption of thymine (DMP): DFT investigations, ChemistrySelect 10 (2025) e02204, https://doi.org/10.1002/slct.202502204.
[83] E.V. Solovyeva, Surface-enhanced Raman scattering: 50 years of development and its role in nanobiotechnology, Nanotechnol. Russia 18 (2024) 1–16, https://doi.org/10.1134/S2635167623601468.
[84] C. Deriu, L. Fabris, A surface chemistry perspective on SERS: revisiting the basics to push the field forward, Chem. Soc. Rev. 54 (2025) 5224–5247, https://doi.org/10.1039/D4CS01242A.
[85] J.S. Al-Otaibi, Y.S. Mary, M. Ismoilov, G. Jhaa, M.C. Gamberini, DFT, spectroscopic and MD insights into teneligliptin (TLG) adsorption on Cu3 and Cu(111): implications for SERS sensing and drug-metal interfaces, Spectrochim. Acta 358 (2026) 127871, https://doi.org/10.1016/j.saa.2026.127871.
[86] J.S. .Al-Otaibi, F.S. Alamro, A.H. Almugrin, Y.S. Mary, G. Jhaa, J.N.C. Mishma, M. S. Roxy, M.C. Gamberini, DFT-driven SERS insight into epoxycyclohexane (CHO) adsorption on Ag20, Au20, and Cu20 nanoclusters for sensing applications, J. Comput. Biophys. Chem. (2027) 1–15, https://doi.org/10.1142/S2737416526500742.